Novel heterogeneous photoredox transformations using organic materials

Cazin, Ines

Master's thesis / Diplomski rad

2017

SVEUČILIŠTE U ZAGREBU

FAKULTET KEMIJSKOG INŽENJERSTVA I TEHNOLOGIJE

SVEUČILIŠNI DIPLOMSKI STUDIJ

Ines Cazin

Nove heterogene fotoreduktivne transformacije organskih materijala/
Novel Heterogeneous Photoredox Transformations Using Organic
Materials

DIPLOMSKI RAD

Voditelj rada: prof. dr. sc. Silvana Raić-Malić

Članovi ispitnog povjerenstva:

1. prof. dr. sc. Silvana Raić-Malić
2. prof. dr. sc. Irena Škorić
3. dr. sc. Petar Kassal

Zagreb, rujan 2017.

This work was performed from

1st March to 1st September 2017

in the Department of Biomolecular Systems

at the Max Planck Institute of Colloids and Interfaces

Acknowledgements

Contents

Summary

Recently, photoredox catalysis has become a popular tool in organic synthesis with a plethora of interesting applications. In 2014, Sammis and co-workers reported decarboxylative fluorination using $Ru(bpy)_3Cl_2$ as a visible-light photoredox catalyst (PRC) in the presence of Selectfluor. More recently (2015), MacMillan and co-workers reported the decarboxylative fluorination with $Ir[dF(CF_3)ppy]_2(dtbbpy)PF_6$. Despite the excellent properties of ruthenium and iridium polypyridyl complexes in PRC, these catalysts are expensive, potentially toxic, and usually not recycled. Compared to these transition metal based homogeneous catalysts, graphitic carbon nitrides (g-C_3N_4) are a class of pure organic, heterogeneous, and therefore, recyclable semiconducting materials with great potential for photoredox catalysis.

The aim of this research is to replace the $Ir[dF(CF_3)ppy]_2(dtbbpy)PF_6$ and $Ru(bpy)_3Cl_2$ catalysts with a modified CMB-C_3N_4 heterogeneous catalyst for the decarboxylative fluorination of carboxylic acids under visible light irradiation at room temperature.

Keywords: photoredox catalysis, semiconducting material, graphitic carbon nitrides (g-C_3N_4), decarboxylative fluorination

1. Introduction

1.1 Photochemistry

Photochemistry describes chemical reactions and physical behavior between atoms or molecules during the exposure with light.[1] In our everyday life, a variety of important processes involve photochemistry. A well-known example is the conversion of carbon dioxide and water into glucose by plants during photosynthesis. Another example includes the formation of vitamin D in the human body.[2]

There are two essential criteria for all photochemical reactions:

1) The starting compound must possess the ability to absorb light;
2) The radiation energy must match the energy difference between the ground and excited state

If we compare a photochemical reaction with a thermal reaction, a difference in nature of excitation is observed. In general, a reaction's transformations are not spontaneous. In order to achieve chemical transformation, there is a need to overcome the activation energy barrier. In the case of thermal reactions, the activation energy is delivered by heat.
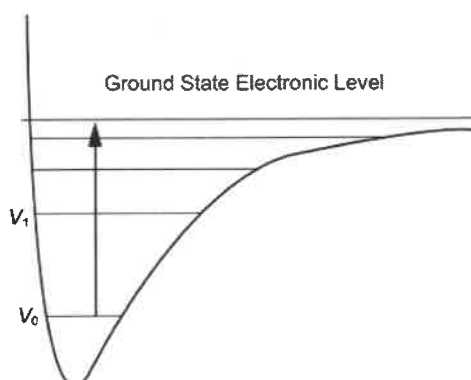

Figure 1 Illustration of thermochemical reaction.

In thermal reactions molecules go to an excited state characterized by higher vibrational energy levels under the influence of heat (Figure 1). Consequently, bond breaking takes places in the first electronic state.

In contrast, in the case of photochemical reactions activation energy is delivered by light. Visible or ultraviolet light give an enormous amount of energy, which leads to electronic excitation and, hence, bond breaking takes place at different electronic levels (Figure 2).
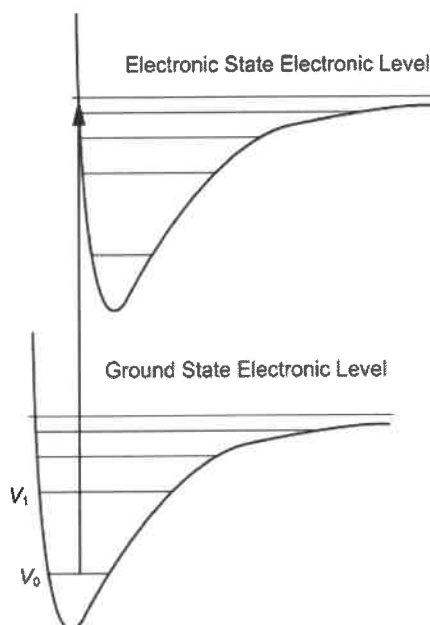
Figure 2 Illustration of photoexcitation.

The energy required for the thermochemical reaction is about 25 kcals. For a photochemical reaction the energy can be calculated as follows:

$$\Delta E = hc/\lambda \qquad \text{(Eq. 1.1)}$$

Energy possessed by the radiation is given as one quantum of energy (hv). If we include in equation 1.1 (Eq. 1.1) the values for Planck's constant (h = $6.625 \cdot 10^{-34}$ Js), speed of light (c = $3.00 \cdot 10^{8}$ m/s), and for example, a wavelength of 10^{-5} cm, we get:

$$\Delta E = 300 \text{ kcals}$$

Along these lines, a thermal reaction involves activation energy in the order of 25 kcal/mole, while photochemical reaction involves activation energy in the order of 100-1000 kcal/mole. Furthermore, the aforementioned equation clearly demonstrates that longer wavelengths are less energetic than shorter wavelengths (Figure 3). [3]
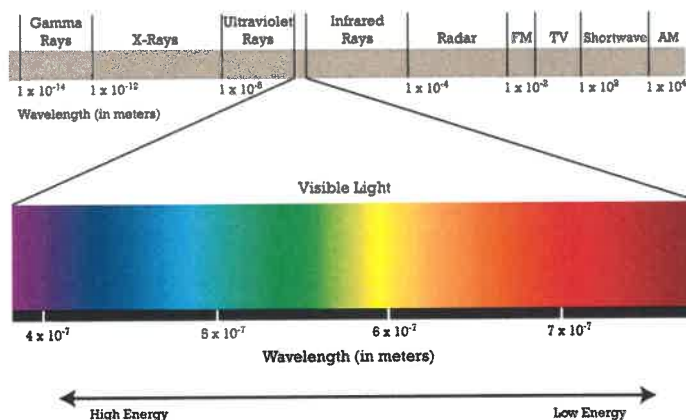
Figure 3 The electromagnetic spectrum.

The different types of electromagnetic radiation shown in Figure 3 are classified into the following classes:

1) Gamma radiation
2) X-ray radiation
3) Ultraviolet radiation
4) Visible radiation
5) Infrared radiation
6) Microwave radiation
7) Radio waves

Consequently, as ultraviolet light (200-400 nm) provides higher activation energy levels (150-70 kcal/mole) when compared to visible light (400-800; 70-40 kcal/mole). It is most often used to produce photochemical change. The temperature has been observed to merely affect the rate of a photochemical reaction. In contrast, it has a significant effect on the rate of a thermochemical reaction. In a photochemical reaction, the intensity of light plays a crucial rule on the reaction rate.

Two basic laws of photochemistry are known:

1) **Grotthus-Draper law** (named after the chemists Christian J.D.T. von Grotthuss and John W. Draper) states that molecules must absorb light in order for a photochemical reaction to take place. Nonetheless, the presence of light alone is not sufficient to induce a photochemical reaction: light should have the correct wavelength to be absorbed by the reactant species.

2) **Starke-Einstein law** (named after physicists Johannes Stark and Albert Einsten) states that only one quantum (or one photon) of light is absorbed by each molecule that undergoes a photochemical reaction. Einstein has concluded this photoequivalence law during his work of the quantum theory of

Table 1 shows the absorption range for some functional groups.

Table 1 Typical absorption ranges for some important functional groups.

Simple alkene	190-200 nm
Acylic diene	220-250 nm
Cyclic diene	250-270 nm
Styrene	270-300 nm
Saturated ketones	270-280 nm
α,β-Unsaturated ketones	310-330 nm
Aromatic ketones/aldehydes	282-300 nm
Aromatic compounds	250-280 nm

When a molecule absorbs light, it undergoes a change in electronic configuration. The Frank-Condon principle states that during light absorption (10^{-5} s) electrons can move, but not the nuclei. This can be explained by the fact that the heavy atomic nuclei do not have the time to readjust themselves during the act of absorption. As a consequence, they have to readjust themselves after the absorption, which swings them into vibration. During excitation the electron spin remains unchanged because spin inversion during excitation is forbidden by quantum mechanics. After the excitation several things may happen.

The most important excited state relaxation processes are:

1) **Fluorescence** (a stimulated and spontaneous emission)
2) **Intersystem crossing** (a jump between the two electronic states with different spin multiplicities)
3) **Internal conversion** (a jump from a higher to a lower electronic state with the same spin multiplicity)
4) **Phosphorescence** (lower energy spontaneous emission occurring from longer-lived excited state, usually triplet multiplicity)
5) **Energy transfer** (excitation transfer)
6) **Photochemical reactions** (photosynthesis, photo-dissociation, photo-induced electron-transfer)
7) **Excited state solvatochromism** (relaxation of molecular excited state caused by strong electric interactions with solvent)

A Jablonski diagram (named after the Polish scientist Alexander Jabłoński) is an energy diagram that can be applied to polyatomic molecules that possess more than one electronic excited state (Figure 5). The diagram illustrates the electronic states of a molecule and the transitions between them. There is one singlet ground state (S0), three singlet excited state (S1, S2, S3), and three triplet excited states (T1, T2, T3).
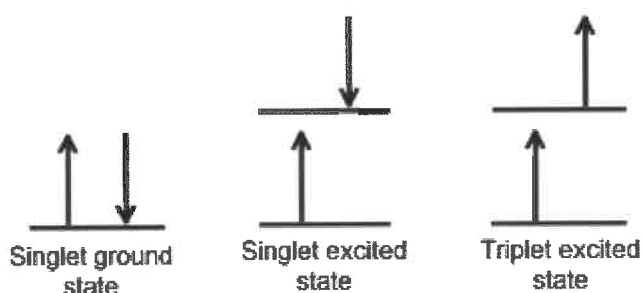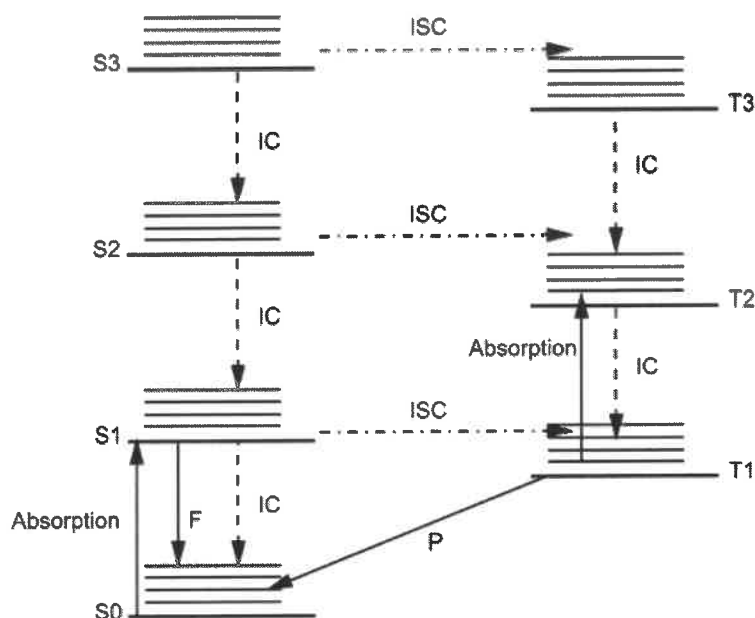

**Figure 4** Singlet and triplet energy levels.

Figure 5 Jablonski Diagram illustrating the photophysical processes such as fluorescence (F), phosphorescence (P), vibrational relaxation, internal conversion (IC), and intersystem crossing (ISC).

Each electronic state has vibrational and rotational states. The molecule is promoted to an excited state by absorption of a photon (indicated by the arrow from S0 to S1 and fluorescence from S1 to S0 is indicated by downward arrow). This stage is not stable and may undergo various physical and chemical processes. For example, the molecule in the first excited state may be converted to a lower vibrational level of the ground state. This process is known as internal conversion (IC). The broken arrow from S1 to T1 indicates intersystem crossing (ISC). It returns to S0 by phosphorescence (P), a process which is indicated by another arrow. The intersystem crossing is shown for S1 to T1, in which the energy level of T1 is lower than the energy level of S1. Furthermore, internal conversion is shown for transition either from a higher singlet state to a lower single state between the same spin multiplicity.[3]

1.1.1 Photoredox catalysis

In recent years, photoredox catalysis has become a powerful strategy for the activation of small molecules. [4] Over the last four decades, advances in photoredox catalysis have enabled the development of a wide array of novel synthetic methodologies. These approaches rely on the ability of organic dyes and metal complexes to convert visible light into chemical energy by engaging in single-electron transfer (SET).[5] The infinitely available, environmentally friendly, and easily handled visible light makes it attractive for chemists to use it in green chemical reactions. Given the advantages abovementioned, photoredox catalysis is widely used in a variety of applications in the realm of carbon dioxide reduction,[6] water splitting,[7] and the development of novel solar cell materials.[8] Recently, its potential in organic synthesis in both industrial and academic settings has been shown. For example, the discovery of new modes of catalysis[9] and advancements in the application of key transformation[10] have provided medicinal chemists access to new chemical space[11] and lead structures that possess a greater diversity when compared to compounds produced via traditional routes.[12]

Potoredox catalysis relies on the ability of the catalyst to act both as an oxidant and as a reductant in its excited states (Figure 6).[13] This means that the photocatalyst can either serve as an electron donor or as an electron acceptor. Upon excitation of the photocatalyst (PCat), an excited species with a higher energy electron (PCat*) is produced, which might be converted into a radical cation (PCat$^{\cdot+}$) through the donation of an electron to the quencher (Q). Subsequently, the cationic species of the photocatalyst (PCat$^{\cdot+}$) accepts an electron from the donor molecule (D) and falls back to the ground state. At this stage, the photocatalytic cycle is completed and ready for the next cycle. This process is known as oxidative quenching.
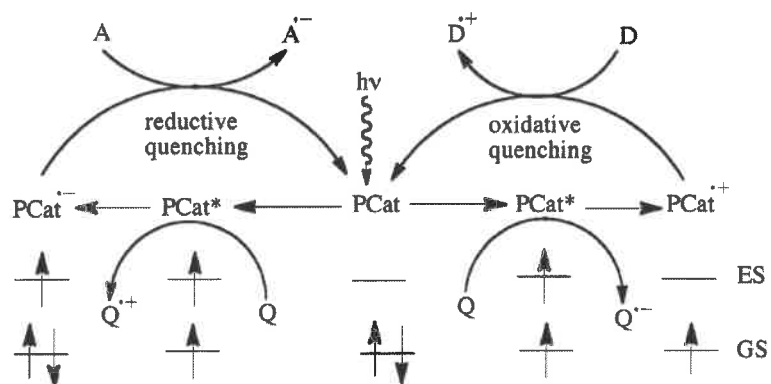
Figure 6 Oxidative and reductive quenching cycles of the photoredox catalyst. PCat = photocatalyst, Q = quencher, D = donor, A = acceptor, GS = ground state, ES = excited state.

Alternatively, reductive quenching can take place. In this, the photo-excited catalyst (PCat*) accepts an electron from the quencher and then donates it to an acceptor molecule (A).

1.1.2 Visible light photoredox catalysis (PRC)

PRC uses visible light as a source of energy to promote electron transfer between reactants in order to result in chemical transformations. To date, the vast amount of visible light photoredox catalysts in organic synthesis is based mostly on two classes of catalysts: transition metal complexes ($Ru(bpy)_3Cl_2$ and $Ir(ppy)_3$) systems and organic dyes (methylene blue or eosin-Y).
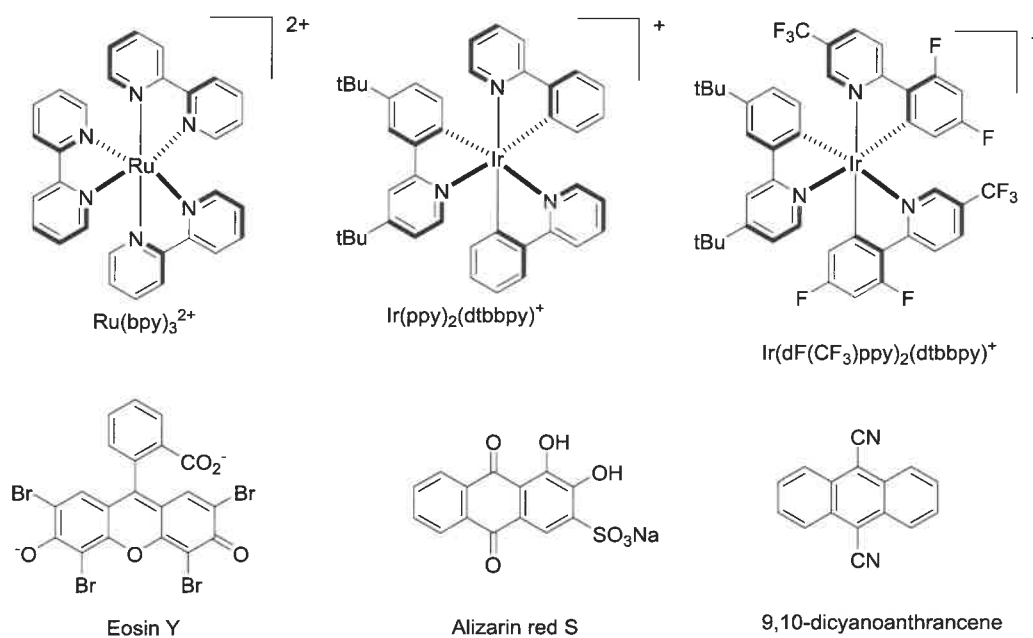
Figure 7 Common photoredox catalysts.

Besides inorganic compounds such as $Ru(bpy)_3Cl_2$ and $Ir(ppy)_2(dtbbpy)PF_6$, organic compounds are also used as visible light photocatalysts. Examples include eosin Y, alizarin red S, 9,10-dicyanoanthrancene (Figure 7).[14]

1.1.3 Ru(bpy)$_3^{2+}$ as a photocatalyst

Ru(bpy)$_3^{2+}$ is the most common and well-studied superior photoredox catalyst[15] because of its absorbance in the visible range (wavelength of 452 nm), unique properties in terms of chemical stability, excited-state lifetimes (originating from metal-to-ligand charge-transfer (MLCT)), and its favorable redox potentials in the excited state, which can be tuned by adjacent ligands[16].

Upon absorption of a photon, an electron in one of the photocatalyst's metal-centered t_{2g} orbitals is excited to a ligand-centered π* orbital. This process is known as metal-to-ligand charge transfer (MLCT) and generates an excited single state. This excited singlet undergoes a rapid intersystem crossing (ISC), and transforms itself into an excited triplet state (see Figure 8).[17] This triplet state is the long-living photoexcited species that engages in the single-electron transfer. The long lifetime can be explained by the fact that the decay to the single ground state is spin-forbidden.
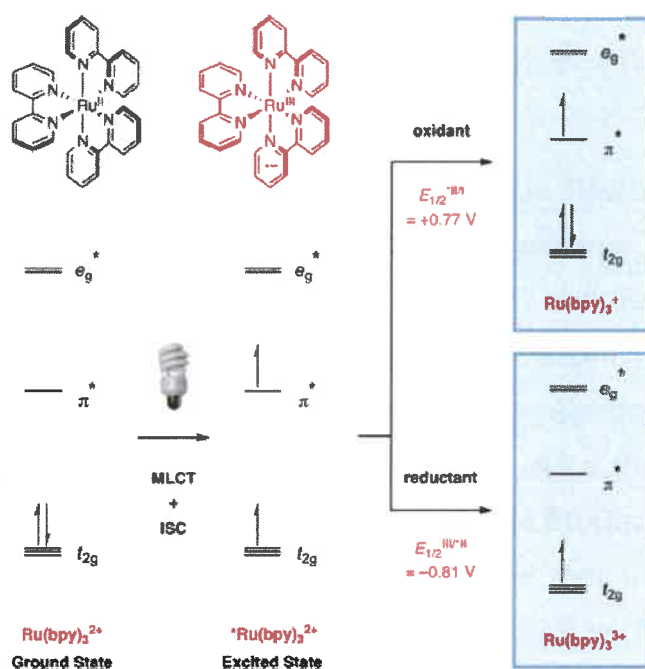
Figure 8 Simplified orbital energy level diagram for the activation of Ru(bpy)$_3^{2+}$.[5]

The excited triplet state, which is generated, is responsible for the excellent reactivity of the catalytic system for two main reasons.[18] First, as mentioned before, the lifetime of the excited triplet state is significantly extended to approximately 1100 ns due to the fact that direct relaxation from an excited triplet state to a ground singlet state is

forbidden (allows intermolecular redox reactions to take place). Secondly, this species can act as a single-electron reductant as well as an oxidant via a single-electron transfer (SET) mechanism.[5]
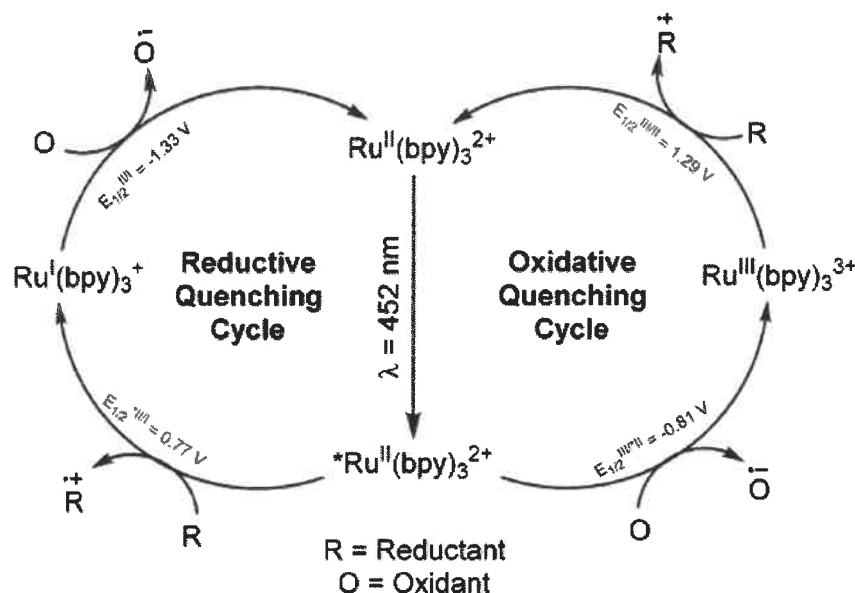

Figure 9 Oxidative and reductive photocatalytic cycles of $Ru(bpy)_3^{2+}$.

As is shown in Figure 9, in the oxidative quenching cycle, $[Ru(bpy)_3]^{2+*}$ functions as a reductant, reducing an electron acceptor by a single electron. The products of this single-electron transfer event are the radical anion of O and the oxidized form of the photocatalyst, $[Ru(bpy)_3]^{3+}$. This species is a strong oxidant ($E_{1/2}^{III/II}$ = +1.29 V *vs.* SCE = Standard Calomel Electrode) and may accept an electron from some donor R to give the radical cation of R and return the catalyst to the Ru(II) ground-state species. Alternatively, in the reducing quenching cycle, $[Ru(bpy)_3]^{2+*}$ functions as an oxidant, accepting an electron from R to generate the reduced species $Ru(bpy)_3^{+}$. This Ru(I) intermediate is a good reductant ($E_{1/2}^{I/II}$ = -1.33 V *vs.* SCE) and may donate an electron to O to generate the ground-state species $Ru(bpy)_3^{2+}$.[19]

1.2 Semi-Conductor Photocatalysis

Homogeneous photoredox catalysts such as $Ru(bpy)_3^{2+}$,[20] Ir^{III} complexes,[21] or Eosin Y[22] have become increasingly popular for their use in PRC during the last couple of years.[23] Despite of their interesting properties, the homogeneous nature of these catalysts hinders both their separation from the end-product and their recycling. From this point of view, heterogeneous recyclable photoredox catalysts provide major advantages.

Figure 10 shows the process involved in semiconductor particles upon bandgap excitation. During the photocatalytic process, the illumination of a semiconductor photocatalyst with visible light activates the catalyst.[24] Semiconductors have a filled valence band (VB) and an empty conduction band (CB).[25] This electronic structure makes them sensitive to light induced redox processes. The band gap is a term that describes the energy difference between the valence and conduction bands.
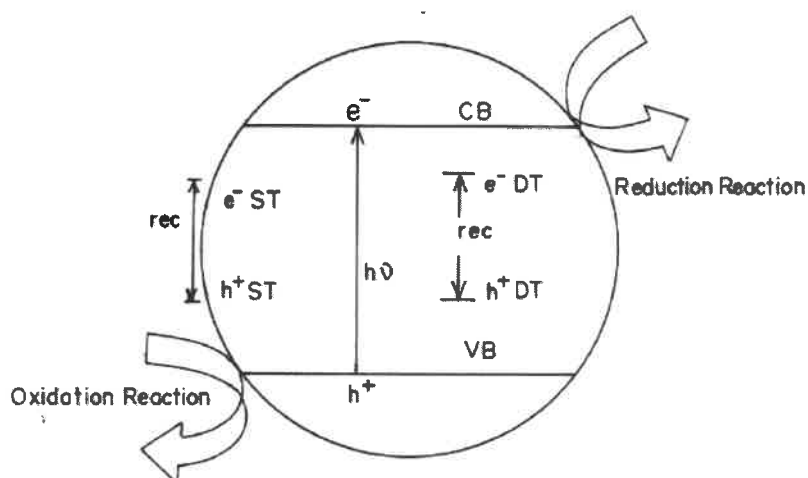
Figure 10 The process involved in semiconductor particles upon bandgap excitation.

The semiconductor photocatalyst absorbs photons with energies equal to or higher than its band gap or threshold energy. Each photon possessing the required wavelength that hits an electron in the occupied valence band of the semiconductor atom can elevate that electron to the unoccupied conduction band leading to the excited state conduction band electrons and positive valence band holes.[26] At this stage, there are three possible mechanistic pathways. The first option is that these charge carriers can get trapped either in shallow traps (ST) or in deep traps (DT). Alternatively, they can recombine non-radiatively or radiatively, dissipating the input

energy as heat. The third possibility is that they can react with electron donors or acceptors adsorbed on the surface of the photocatalyst. However, recently it was shown that any photo-redox chemistry occurring at the particle surface emanates from trapped electrons and trapped holes rather than from free valence band holes and conduction band electrons.[27]

1.2.1 Graphitic carbon nitride

Recently, graphitic carbon nitride (g-C_3N_4) has emerged as a promising visible-light-responsive polymeric photocatalyst since it is cheap, metal-free, and recyclable.[28] Density functional theory (DFT) simulations have provided evidence that carbon-doped g-C_3N_4 show a thermodynamically stable structure, promoted charge separation, and had suitable energy levels of conduction and valence bands for photocatalytic oxidation when compared to phosphorus-doped g-C_3N_4. Moreover, the optimized carbon-doped g-C_3N_4 showed faster reaction rates for some transformations compared to conventional g-C_3N_4.[29]
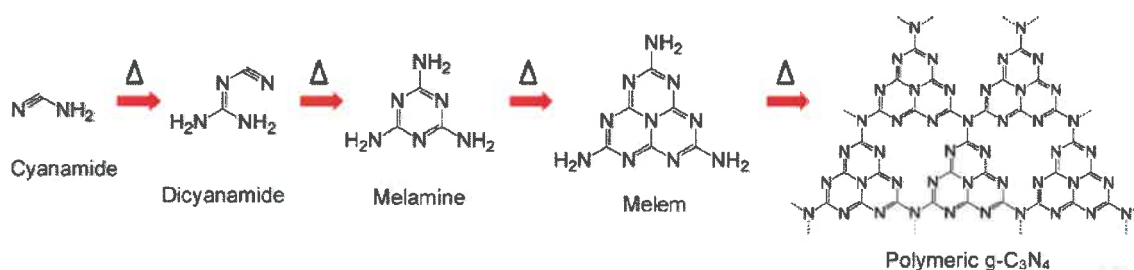

Figure 11 Preparation of g-C_3N_4.

In this thesis, photoredox transformations were performed by using modified carbon nitride CMB-C_3N_4. The supramolecular complex (CMB-C_3N_4) was prepared by the pyrolysis of cyanuric acid (C), melamine (M), and barbituric acid (B) (Figure 12). C_3N_4 materials have already been applied in various ways such as catalysts in heterogeneous catalysis, as metal free photocatalysts, and as electrocatalysts in water splitting reactions.[30-31] This material possesses excellent chemical and photophysical properties such as high chemical and thermal stability (up to 400 °C) as well as suitable properties for water splitting under illumination (both proton reduction and water oxidation). Considering the strong dependence of the

photocatalytic activity of C_3N_4 on its morphology, surface area, size, defect, and energy states along with its electronic properties, there are several modified graphitic carbon nitrides.[32]
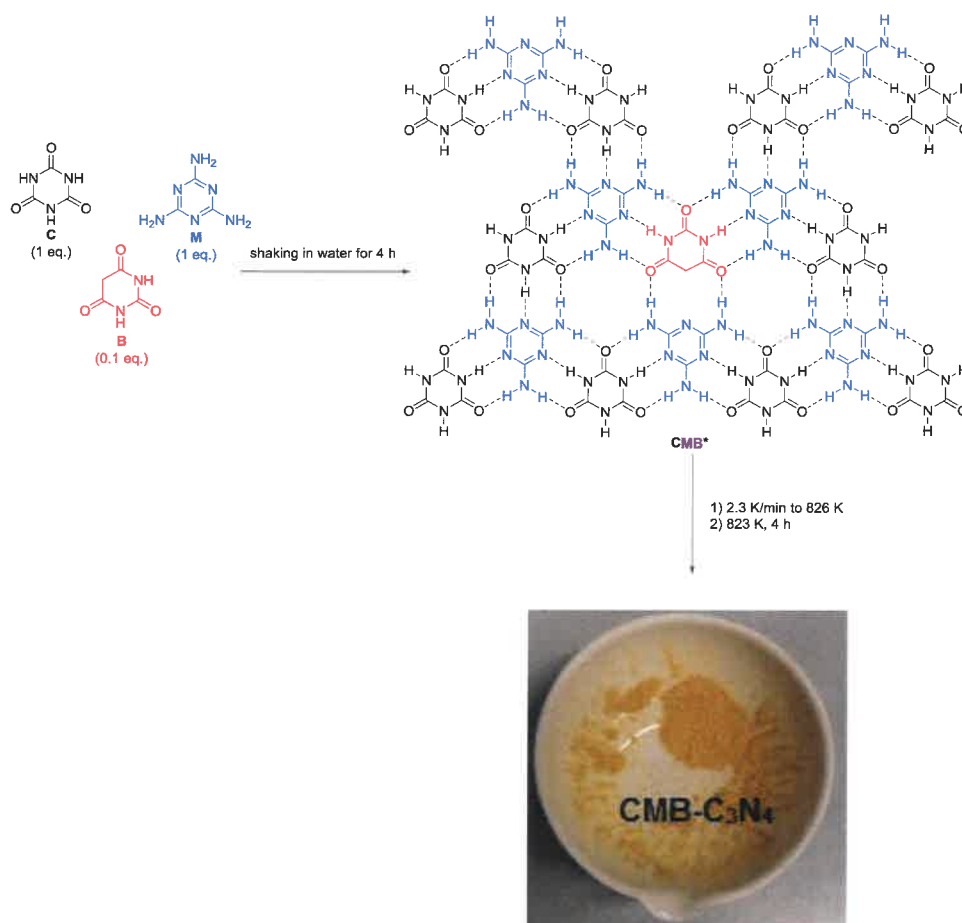

Figure 12 Preparation of CMB-C_3N_4.

1.3 Visible-light photoredox mediated decarboxylative couplings

Carboxylic acids are moieties that are widely observed in organic molecules and natural products.[33] They are abundant and inexpensive organic and biomass-derived platform molecules, and their conversion into high-value products has attracted much attention. Visible-light photoredox decarboxylative coupling reactions have become important chemical transformations because of their wide substrate scope, mild reaction conditions, high efficiency, and practicability.[34]
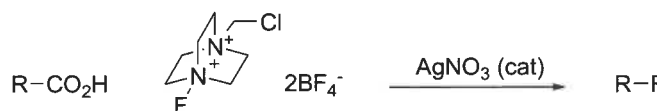
1.3.1 Decarboxylative fluorination

The increasing importance of fluorinated compounds in the pharmaceutical, agrochemical, and polymer industries has placed a premium on the development of new methods for carbon-fluorine bond formation under mild conditions.[35-36] While methods for sp^3 C-F formations have been developed[37-39], the formation of sp^2 C-F bonds is still challenging. Elegant examples included deoxofluorination of phenol,[40] fluorination of aryl trifluoroborates,[41-42] and bromo/triflate-fluorine exchange.[43-44] The use of the other common C(sp^2) functionalities, such as widely available carboxylic acid, are still missing.
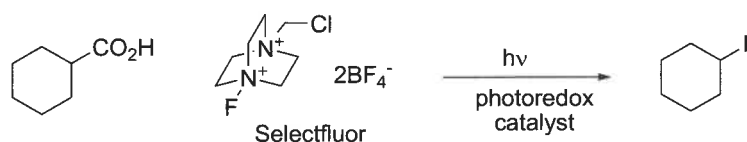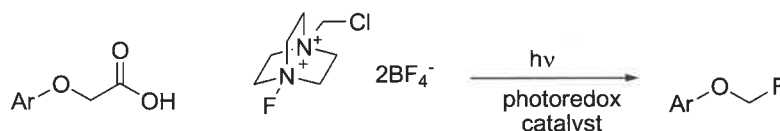

Figure 13 Recent advances in decarboxylative fluorination.

Recently, several examples of decarboxylative fluorination have been reported (Figure 13). For example, Li and co-workers have reported a silver-catalyzed radical decarboxylative fluorination of organic acids.[45] Sammis and co-workers have reported a decarboxylative fluorination by using $Ru(bpy)_3Cl_2$ as a photocatalyst in the presence of Selectfluor.[46] Very recently, MacMillan and co-workers have reported an elegant way of decarboxylative fluorination of aliphatic carboxylic acid with $Ir[df(CF_3)ppy]_2(dtbbpy)PF_6$ in the presence of Selectfluor.[47]

2. Results and discussion

My study commenced with the model reaction between phenylacetic acid (**1**) and Selectfluor (Scheme 1). The light source used for the photoreactions was a flexible 5 meter, red/green/blue 24 W LED band purchased in Bauhaus.
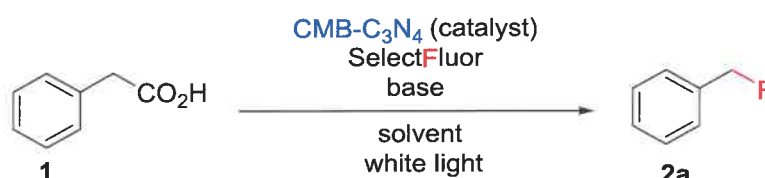
Scheme 1. Decarboxylative fluorination of phenylacetic acid (**1**) using CMB-C_3N_4.

After studying the literature for suitable solvents and bases, I decided to start the reaction optimization with the solvent mixture of acetonitrile (MeCN) and water (H_2O). The next step was an investigation for a suitable solvent ratio. Obtaining a homogeneous reaction mixture was difficult because of the solubility of the reagents. Selectfluor is poorly soluble in MeCN while the carboxylic acid is insoluble in water. A solvent ratio of 1:9 (MeCN:H_2O) resulted in a homogeneous mixture.

Next, various bases were screened (Table 2). Carbonate-containing bases such as sodium hydrogen carbonate ($NaHCO_3$), sodium carbonate (Na_2CO_3) and calcium carbonate ($CaCO_3$) produced similar or slightly higher yield than caesium carbonate (Cs_2CO_3). Sodium hydroxide (NaOH), a strong base, gave 22 % yield (entry 9). The use of caesium acetate (CsOAc) and 1,8-Diazabicyclo[5.4.0]undec-7-ene (DBU) resulted in no reaction (entries 11 and 12). Further optimization with different sodium, lithium, potassium and caesium bases revealed that caesium fluoride (CsF) was the best with 89 % yield (entry 10).

Table 2 Base screening in the decarboxylative fluorination of phenylacetic acid (**1**) using CMB-C_3N_4.
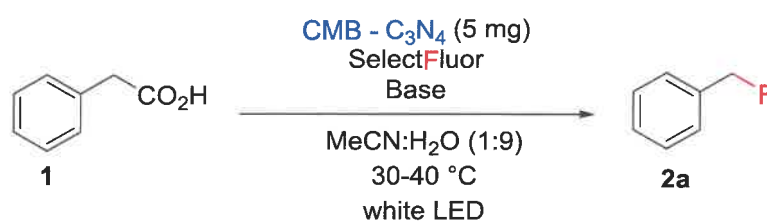
entry	base	NMR yield [%]
1	Na_2HPO_4	57
2	K_2HPO_4	28
3	$NaHCO_3$	30
4	Cs_2CO_3	23
5	$CaCO_3$	35
6	Na_2CO_3	41
7	LiOH	8
8	KOH	11
9	NaOH	22
10	CsF	89
11	CsOAc	0
12	DBU	0
13	2,6-lutidine	27

Conditions: **1** (1 equiv., 0.4 mmol), Selectfluor (3 equiv., 1.2 mmol), base (2 equiv., 0.8 mmol) in 2 mL of MeCN:H_2O (0.2 M). NMR yields determined by ^{19}F-NMR with 2,2,2-trifluorethanol according to the general procedure. Reaction time 4 h.

Table 3 Reduction of base and Selectfluor equivalents for the decarboxylative fluorination of phenylacetic acid (**1**) using CMB-C$_3$N$_4$.
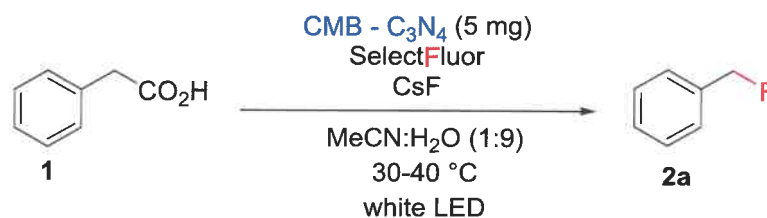
entry	equiv. CsF	equiv. Selectfluor	NMR yield [%]
1[a]	2	1.5	24
2[b]	1	3	47

Conditions: [a]**1** (1 equiv., 0.4 mmol), Selectfluor (1.5 equiv., 0.6 mmol), CsF (2 equiv., 0.8 mmol) in 2 mL of MeCN:H$_2$O (0.2M). [b]**1** (1 equiv., 0.4 mmol), Selectfluor (3 equiv., 1.2 mmol), CsF (1 equiv., 0.4 mmol) in 2 mL of MeCN:H$_2$O (0.2 M). NMR yields determined by ^{19}F-NMR with 2,2,2-trifluorethanol as an internal standard according to the general procedure. Reaction time 4 h.

As is shown inTable 3, reduction of Selectfluor (entry 1) resulted in a significantly lower yield. A similar result was observed when the equivalents of CsF were reduced (entry 2), where incomplete conversion occurred.

Table 4 Reaction time optimization for the decarboxylative fluorination of phenylacetic acid (**1**) using CMB-C3N4.

CMB - C_3N_4 (5 mg)
SelectFluor)
CsF

MeCN:H_2O (1:9)
30-40 °C
white LED

1 → **2a**
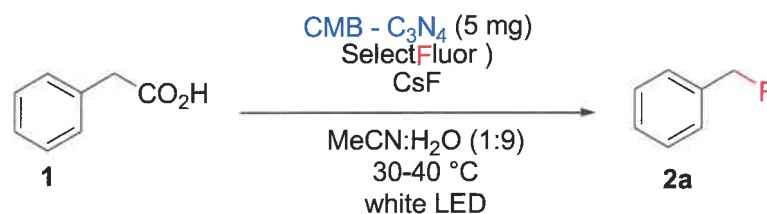
entry	irradiation time [h]	NMR yield [%]	1:2a
1	2	32	1.5:1
2	3	60	0.6:1
3	4	89	0

Conditions: **1**(1 equiv., 0.4 mmol), Selectfluor (3 equiv., 1.2 mmol), CsF (2 equiv., 0.8 mmol) in 2 mL of MeCN:H_2O (0.2 M). NMR yields determined by ^{19}F NMR with 2,2,2-trifluorethanol as an internal standard and **1:2a** ratios by ^{1}H NMR according to the general procedure.

The effect irradiation time has on conversion and yield is shown in **Error! Reference ource not found.**. The substrate-to-product ratio shows full conversion within 4 hours.

The use of mesoporous graphitic carbon nitride (mpg-C_3N_4) resulted in slower conversion (Table 5) and therefore CMB-C_3N_4 was used in all further studies.

Table 5 Catalyst studies for the decarboxylative fluorination of phenylacetic acid (**1**).
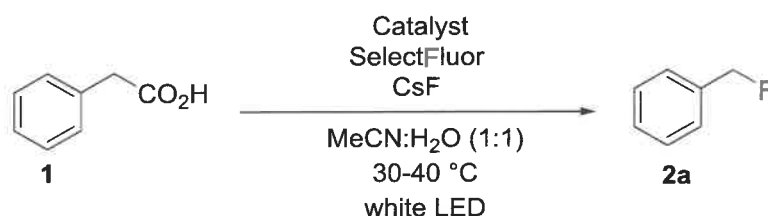
entry	catalyst	1:2a
1	CMB – C_3N_4	0.3:1
2	mpg-C_3N_4	9.5:1

Conditions: Catalyst (5 mg), **1** (1 equiv., 0.4 mmol), Selectfluor (3 equiv., 1.2 mmol), CsF (2 equiv., 0.8 mmol) in 2 mL of MeCN:H_2O (0.2 M). **1:2a** ratios were determined by ^{1}H-NMR according to the general procedure. Reaction time 2 h.

Table 6 shows the results of testing different concentrations and solvent ratios. The solvent ratio had a significant impact on the reaction rate and a 1:1 mixture gave full conversion within 4 h (entry 1). More acetonitrile or water in the reaction mixture resulted in slower reaction rates (entries 2 and 4). Surprisingly, there is a significantly huge difference between NMR yield and substrate-to-product ratio (**1:2a**) for the same entries, especially for the entry 3. These results, thus, need to be interpreted cautiously.

Table 6 Solvent ratio studies of the decarboxylative fluorination of phenylacetic acid (**1**) using CMB-C3N4.
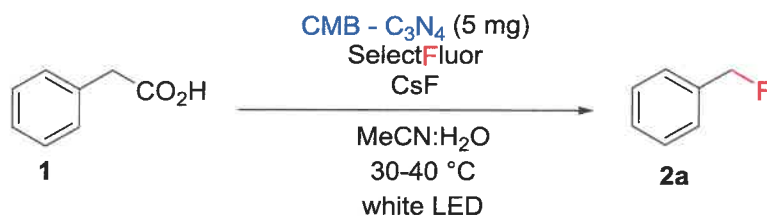
entry	MeCN:H_2O	c [M]	NMR yield [%]	1:2a
1[a]	1:1	0.2	94	0.1:1
2[a]	1:9	0.2	87	0.1:1
3[b]	1:1	0.1	57	0
4[c]	2:1	0.13	13	1.4:1

Conditions: [a]**1**(1 equiv., 0.4 mmol), Selectfluor (3 equiv., 1.2 mmol), CsF (2 equiv., 0.8 mmol) in 2 mL of MeCN:H_2O (0.2 M). [b]**1**(1 equiv., 0.4 mmol), Selectfluor (3 equiv., 1.2 mmol), CsF (2 equiv., 0.8 mmol) in 4 mL of MeCN:H_2O (0.1 M). [c]**1**(1 equiv., 0.4 mmol), Selectfluor (3 equiv., 1.2 mmol), CsF (2 equiv., 0.8 mmol) in 3 mL of MeCN:H_2O (0.13 M). NMR yields determined by ^{19}F-NMR with 2,2,2-trifluorethanol as an internal standard and 1:2a ratios by ^{1}H-NMR according to the general procedure. Reaction time 4 h.

Due to the discrepancy observed in Table 6, the procedure for the determining NMR yields and substrate-to-product ratios was examined in closer detail. As in Table 6, Table 7 clearly demonstrates the problem with using the internal standard chosen for NMR yield determination. The same conditions were tested twice and showed that the yields were not reproducible for identical conditions (entries 1 and 2) using ^{19}F-NMR with 2,2,2-trifluorethanol as an internal standard. On the other hand, no significant differences were found between results of **1:2a** ratios by ^{1}H-NMR. The reaction reproducibility is probably not the problem but the method for determining yield.

Table 7 Reproducibility studies for NMR yields and substrate-to-product ratios of the decarboxylative fluorination of phenylacetic acid (**1**) using CMB-C_3N_4.
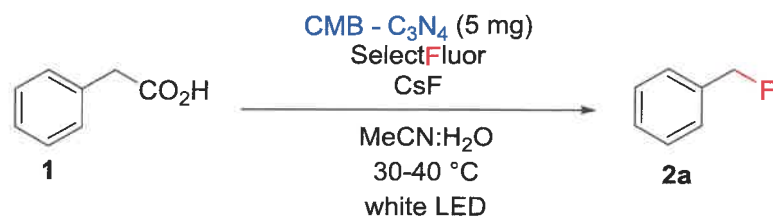

entry	solvent ratio	NMR yield [%]	1:2a
1	1:1	93	0.4:1
2	1:1	52	0.9:1
3	2:1	44	1.5:1
4	2:1	35	1.6:1
5	1:2	72	0.5:1
6	1:2	44	0.7:1
7	1:9	30	1.6:1
8	1:9	20	2.1:1

Conditions: **1** (1 equiv., 0.4 mmol), Selectfluor (3 equiv., 1.2 mmol), CsF (2 equiv., 0.8 mmol) in 2 mL of MeCN:H_2O (0.2 M). NMR yields determined by ^{19}F-NMR with 2,2,2-trifluorethanol as an internal standard and 1:2a ratios by ^{1}H-NMR according to the general procedure. Reaction time 2 h.

This irreproducibility can be rationalized by the of 2,2,2-trifluorethanol. Possibly, the internal standard responds to reaction mixture characteristics such as analytes in the organic and aqueous phase. This means that NMR yield is not accurate because one equivalent of the internal standard is not present in the organic phase. This problem was circumvented by using a less polar internal standard (α,α,α-trifluorotoluene) with lower volatility in comparison to 2,2,2-trifluorethanol. The next step was testing α,α,α-trifluorotoluene.

Table 8, replacing 2,2,2-trifluorethanol with α,α,α-trifluorotoluene resulted in NMR yields and 1:2a ratios which were more sensible. For example, low yields resulted in high **1:2a** ratios while high yields resulted in low **1:2a** ratios. The hypothesis that a high-boiling, less polar internal standard should improve the reproducibility was correct. Also, the lamp described in the beginning of these studies was replaced with the new one with the same properties but further experiments revealed that the second lamp resulted in slower transformations for the same conditions.

Table 8 Internal standard studies for determining the NMR yield of the decarboxylative fluorination of phenylacetic acid (**1**) using CMB-C_3N_4.
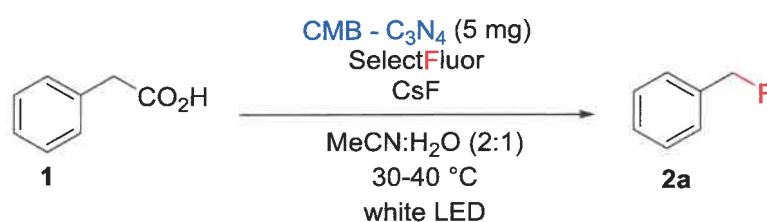

entry	reaction time [h]	NMR yield [%]	1:2a
1	2	13	7.4:1
2	4	39	1.4:1
3	6	55	0.6:1
4	8	60	0.3:1
5	15	74	0.1:1

Conditions: **1** (1 equiv., 0.4 mmol), Selectfluor (3, equiv., 1.2 mmol), CsF (2 equiv., 0.8 mmol) in 2 mL of MeCN:H_2O (0.2 M). NMR yields determined by ^{19}F-NMR with α,α,α-trifluorotoluene as an internal standard and **1:2a** ratios by ^{1}H-NMR according to the general procedure.

As mentioned above, the use of lamps with the same specifications does not give the same results. Several bases from the Table 1 were screened with the new lamp (Table 9).

Table 9 Base studies of the decarboxylative fluorination of phenylacetic acid (**1**) using CMB-C_3N_4 with the new lamp.
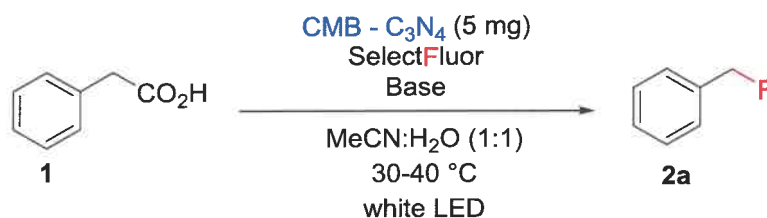
entry	base	NMR yield [%]	1:2a
1	CsF	48	0.9:1
2	Na_2HPO_4	21	4.1:1
3	NaH_2PO_4	24	3.3:1
4	Cs_2CO_3	10	11.6:1
5	2,6-lutidine	43	0.85:1
6	CsOAc	0	0
7	KOH	0	0
8	K_2HPO_4	18	4.8:1

Conditions: **1** (1 equiv., 0.4 mmol), Selectfluor (3 equiv., 1.2 mmol), CsF (2 equiv., 0.8 mmol) in 3 mL of MeCN:H_2O (0.13 M). NMR yields determined by ^{19}F-NMR with α,α,α-trifluorotoluene as an internal standard and **1:2a** ratios by ^{1}H-NMR according to the general procedure. Reaction time 4 h.

The optimized conditions described above were subsequently applied in the decarboxylative fluorination of phenylacetic acid (**1**) using a new lamp. As expected, cesium fluoride (CsF) was the best base with 48 % NMR yield but in significantly lower yield and conversion than in Table 5 (entry 1) where 94 % NMR yield was observed within 4 hours. Furthermore, the use of 2,6-lutidine resulted in three additional fluorination products (unidentified) observed by NMR analysis.

Table 10 Solvent ratio and concentration studies of the decarboxylative fluorination of phenylacetic acid (**1**) using CMB-C_3N_4.
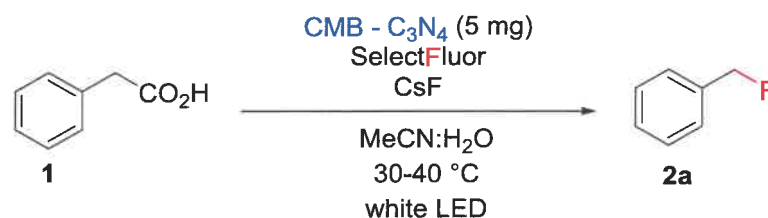

entry	c [M]	solvent ratio	NMR yield [%]	1:2a
1[a]		1:1	48	0.9:1
2[a]	0.13	2:1	29	2.8:1
3[a]		1:2	34	1.5:1
4[b]		1:1	47	0.7:1
5[b]	0.2	2:1	37	1.8:1
6[b]		1:2	28	2.5:1

Conditions: [a]**1** (1 equiv., 0.4 mmol), Selectfluor (3 equiv., 1.2 mmol), CsF (2 equiv., 0.8 mmol) in 3 mL of MeCN:H_2O (0.13 M). [b]**1** (1 equiv., 0.4 mmol), Selectfluor (3 equiv., 1.2 mmol), CsF (2 equiv., 0.8 mmol) in 2 mL of MeCN:H_2O (0.2 M). NMR yields determined by ^{19}F-NMR with α,α,α- trifluorotoluene as an internal standard and **1:2a** ratios by ^{1}H-NMR according to the general procedure. Reaction time 4 h.

As is shown in Table 10, there is no big difference in results between concentrations (0.13 and 0.2 M), but the solvent ratio was found to have a significant impact on the reaction rate (entries 1 and 3).

NMR analysis (Table 11) showed that the solvent ratio of acetonitrile and water (1:1) at a concentration of 0.13 M gave almost full conversion within 15 hours (entry 9).

Table 11 Time optimization for the decarboxylative fluorination of phenylacetic acid (**1**) using CMB-C_3N_4.
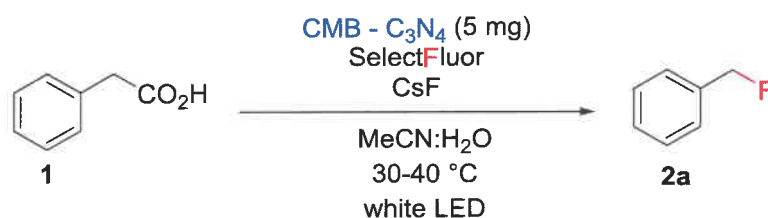
entry	MeCN:H_2O	irradiation time [h]	NMR yield [%]	1:2a
1		2	13	7.4:1
2		4	29	2.8:1
3	2:1	6	55	0.6:1
4		8	60	0.3:1
5		15	74	0.1:1
6		4	48	0.9:1
7	1:1	6	67	0.4:1
8		8	63	0.4:1
9		15	82	0.03:1

Conditions: **1** (1 equiv., 0.4 mmol), Selectfluor (3 equiv., 1.2 mmol), CsF (2 equiv., 0.8 mmol) in 3 mL of MeCN:H_2O (0.13 M). NMR yields determined by ^{19}F-NMR with α,α,α-trifluorotoluene as an internal standard and **1:2a** ratios by ^{1}H-NMR according to the general procedure.

Alternative electrophilic fluorination reagents, such as 1-fluoropyridium tetrafluoroborate (NFPY, entry 1) and *N*-fluorobenzenesulfonimide (NSFI, entry 2) were also tested. However, neither afforded the desired product or any conversion at all (Table 12). This showcases the uniqueness of Selectfluor for this transformation.

Table 12 Test of alternative electrophilic fluorination reagents.

CMB - C_3N_4 (5 mg)
Fluorination reagent
CsF

MeCN:H_2O (1:1)
30-40 °C
white LED

1 → **2a**
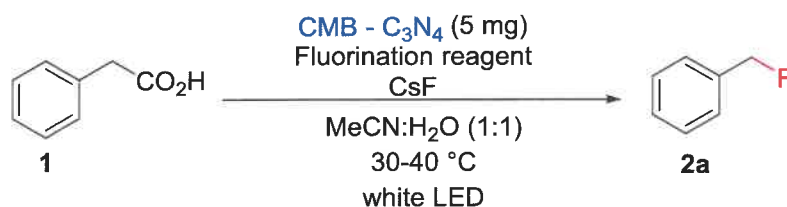
entry	fluorination reagent	NMR yield [%]
1[a]	BF_4^- (N-fluoropyridinium)	0
2[b]	(NFSI structure)	0

Conditions: [a]**1** (1 equiv., 0.4 mmol), NFPY (3 equiv., 1.2 mmol), CsF (2 equiv., 0.8 mmol) in 3 mL of MeCN:H_2O (0.13 M). [b]**1** (1 equiv., 0.4 mmol), NFSI (3 equiv., 1.2 mmol), CsF (2 equiv., 0.8 mmol) in 3 mL of MeCN:H_2O (0.13 M). NMR yields determined by ^{19}F NMR with α,α,α- trifluorotoluene as an internal standard according to the general procedure. Reaction time 15 h.

Figure 14 Reaction mixtures with NFPY (left), NSFI (middle) and Selectfluor (right).

Control experiments are shown in Table 13. In the absence of the heterogeneous photoredox catalyst or light, no reaction occurred (entries 4 and 5). Without a base a very slow reaction was observed (entry 3).

Table 13 Control studies of the decarboxylative fluorination of phenylacetic acid (**1**) using CMB-C_3N_4.
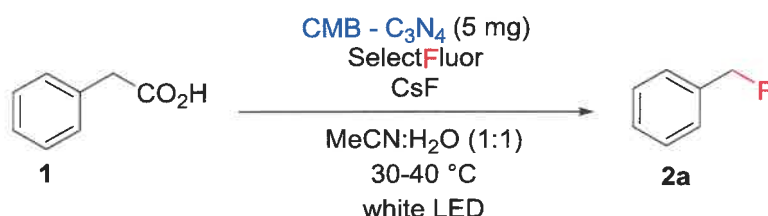
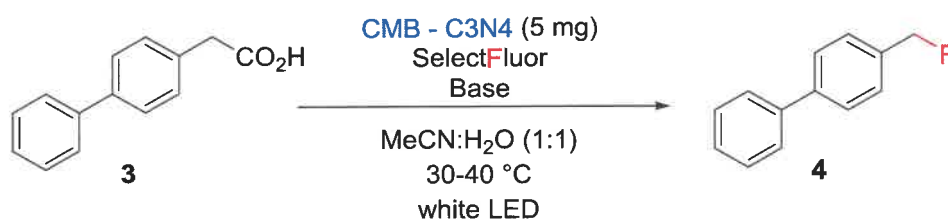| entry	conditions	NMR yield [%]	1:2a
1	as shown	82	0.03:1
2	without degassing	0	0
3	without CsF	12	5.0:1
4[a]	without light	0	0
5	without catalyst	0	0

Conditions: **1** (1 equiv., 0.4 mmol), Selectfluor (3 equiv., 1.2 mmol), CsF (2 equiv., 0.8 mmol) in 3 mL of MeCN:H_2O (0.13 M). NMR yields determined by ^{19}F-NMR with α,α,α-trifluorotoluene as an internal standard and **1:2a** ratios by ^{1}H-NMR according to the general procedure. [a]The reaction was covered in aluminium foil. Reaction time 15 h.

Finally, reactions using acetone:H_2O were tested and gave similar results to those using MeCN:H_2O. The desired product was not formed, however, when a mixture of DMF:H_2O was used (Table 14).

Table 14 Solvent studies of the decarboxylative fluorination of the phenylacetic acid (**1**) using CMB-C_3N_4.
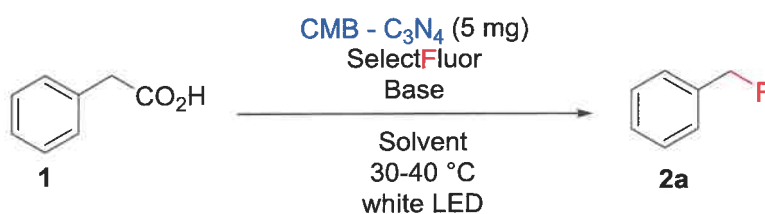
entry	base	solvent ratio	NMR yield [%]	1:2a
1	CsF	MeCN:H_2O 1:1	94	0.1:1
2	Na_2HPO_4	DMF:H_2O 1:1	0	0
3	Na_2HPO_4	acetone:H_2O 3:7	27	1.7:1
4	CsF	acetone:H_2O 1:1	78	0.05:1

Conditions: **1** (1 equiv., 0.4 mmol), Selectfluor (3 equiv., 1.2 mmol), base (2 equiv., 0.8 mmol) in 2 mL of MeCN:H_2O (0.2 M). NMR yields determined by ^{19}F-NMR with 2,2,2-trifluorethanol as an internal standard and **1:2a** ratios by ^{1}H-NMR according to the general procedure. Reactions performed with the first lamp. Reaction time 4 h.

Generally, the optimal combination of base and solvent mixture was the key for this reaction. It was found that simply mixing **1** with Selectfluor at the room temperature in acetonitrile (MeCN) and water (1:1) afforded 82 % NMR yield within 15 hours.

With the optimized conditions for phenylacetic acid (**1**) in hand, the next step was the investigation of decarboxylative fluorination of 4-biphenylacetic acid (**3**).

The conditions described above were subsequently applied to the decarboxylative fluorination of 4-biphenylacetic acid (Table 14), however, resulted in significantly lower yields (entry 1). As mentioned, the use of 2,6-lutidine resulted in three additional fluorination products (unidentified) observed by NMR analysis (entry 2).

Table 15 Base studies for the decarboxylative fluorination of 4-biphenylacetic acid (**3**) using CMB-C_3N_4.

entry	base	NMR yield [%]	3:4
1	CsF	42	1.4:1
2	2,6-lutidine	54	0.9:1
3	Cs_2CO_3	12	4.8:1
4	NaOH	26	2.8:1
5	K_2HPO_4	38	1.4:1
6	NaH_2PO_4	8	10.2:1
7	Na_2HPO_4	32	1.8:1

Conditions: **3** (0.4 mmol), Selectfluor (1.2 mmol), base (0.8 mmol) in 2 mL of MeCN:H_2O (0.2 M). NMR yields determined by ^{19}F-NMR with 2,2,2-trifluorethanol as an internal standard and **3:4** ratios by ^{1}H-NMR according to the general procedure. Reaction time 4 h. Reactions performed with the first lamp.

The resulting mixture of the reactions from the Table 15 with CsF and K_2HPO_4 were biphasic. This is most likely caused by the nonpolar product and the higher concentration of product. It is hypothesized that this phenomenon causes the decreased reaction rate.

Table 16 Solvent ratio and concentration studies of the decarboxylative fluorination of 4-biphenylacetic acid (**3**) using CMB-C_3N_4.
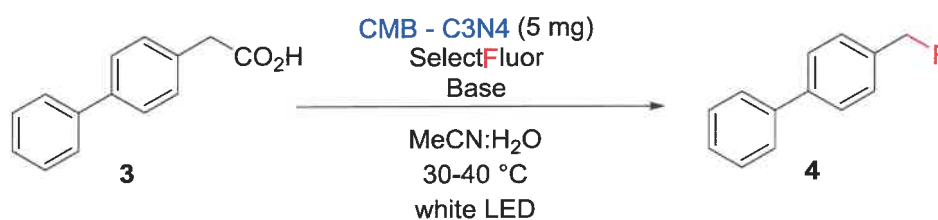
entry	base	solvent ratio	c [M]	3:4
1		1:1	0.2	0.5:1
2[b]		1:2	0.2	0.7:1
3	CsF	1:1	0.1	0.6:1
4[a,c]		1:1	0.1	1.3:1
5[d]		1:2	0.1	27.9:1
6		1:1	0.13	0.1:1
7[b]		1:1	0.2	1.1:1
8[b]	K_2HPO_4	1:1	0.1	0.9:1
9[e]		1:1	0.13	0.7:1
10[d]	2,6-lutidine	1:2	0.1	1.7:1

Conditions: **3** (1 equiv., 0.4 mmol), Selectfluor (3 equiv., 1.2 mmol), base (2 equiv., 0.8 mmol) in 2, 3 and 4 mL of MeCN:H_2O (0.2, 0.13 and 0.1 M). [a]Reaction time 4 h. [b]Reaction time 17 h. [c]**3** (0.7 mmol), Selectfluor (2 equiv., 1.4 mmol), base (2 equiv., 1.4 mmol) in 7 mL of MeCN:H_2O (0.1 M). [d]**3** (1 equiv., 0.2 mmol), Selectfluor (3 equiv., 0.6 mmol), base (2 equiv., 0.4 mmol) in 2 mL of MeCN:H_2O (0.1 M). [e]**3** (1 equiv., 0.4 mmol), Selectfluor (2 equiv., 0.8 mmol), base (1 equiv., 0.4 mmol) in 2 mL of MeCN:H_2O. **3:4** ratios determined by ^{1}H-NMR according to the general procedure. Reaction time 16 h. Reactions performed with the first lamp.

The reactions from the Table 16 were performed at different concentrations and solvent ratios in order to find the optimal condition for which no biphasic reaction mixture resulted. While different concentrations (using CsF as the base, entries 1 and 3) of the same solvent ratio (1:1) did not result in a significant difference between the substrate-to-product ratio, a biphasic nature of both reaction mixture was observed. (Figure 15).
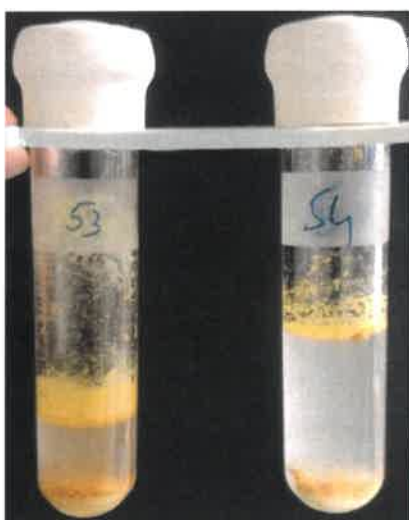
Figure 15 The resulting mixtures of 0.1 M (left) and 0.2 M (right) with a solvent ratio of 1:1 with CsF as base.

Similar results were found for the reactions performed with K_2HPO_4 as base (entries 7 and 8). Both reactions resulted in slower reaction rates with the biphasic reaction mixture (Figure 16).

Figure 16 The resulting mixtures of 0.1 M (left) and 0.2 M (right) concentrations with a solvent ratio of 1:1 with K_2HPO_4 as base.

Interestingly, when the reaction (entry 4) was performed on the larger scale with 0.7 mmol of 4-biphenylacetic acid (**3**) and the same equivalents of Selectfluor and base (2 equiv), a 1.3:1 substrate-to-product ratio resulted within 4 hours. Unfortunately, the reaction mixture was biphasic (Figure 17).

Figure 17 The resulting mixtures at 0.1 M with reduced Selectfluor.

Along these lines, the reaction which was carried out on a smaller scale with 0.2 mmol of **3** (entry 5) resulted in very slow reaction rate (27.9:1 substrate-to-product ratio).

Table 17 Solvent studies of the decarboxylative fluorination of 4-biphenylacetic acid (**3**) using CMB-C_3N_4.
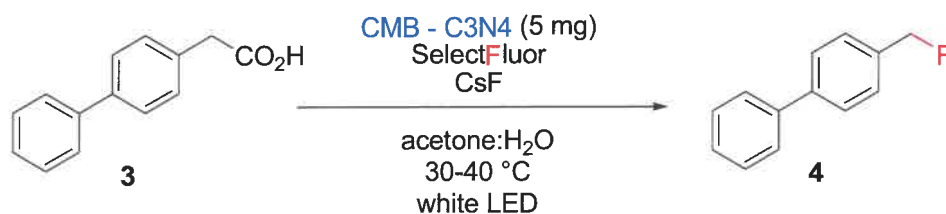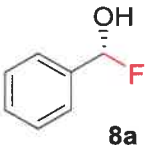

entry	solvent ratio	3:4
1	1:1	1.1:1
2	1:2	2.2:1
3[a,b]	2:1	0.3:1

Conditions: **3** (1 equiv., 0.4 mmol), Selectfluor (3 equiv., 1.2 mmol), base (2 equiv., 0.8 mmol) in 2 mL of MeCN:H_2O (0.2 M). [a]**3** (1 equiv., 0.4 mmol), Selectfluor (3 equiv., 1.2 mmol), base (2 equiv., 0.8 mmol) in 3 mL of MeCN:H_2O (0.13 M). [b]Reaction time 7 h. Reaction time 17 h. **3:4** ratios determined by ^{1}H-NMR according to the general procedure.

Encouragingly, reactions tested with acetone as a solvent ratio of 2:1 at 0.13 M gave a 0.3:1 substrate-to-product ratio within 7 hours (entry 3).

a)   b)
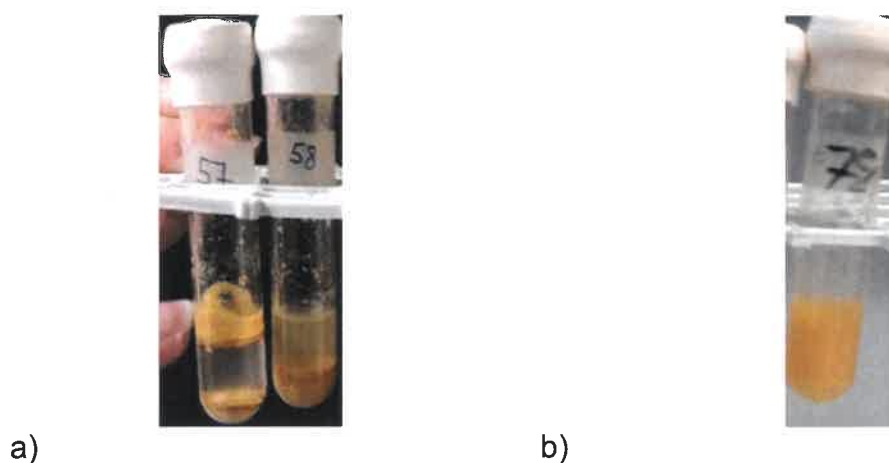
Figure 18 The resulting mixtures. a) 0.1 M with a solvent ratio of 1:1 (left) and 1:2 (right). b) 0.13 M with an optimal solvent ratio 2:1.

Table 18 Reaction optimization for the decarboxylative fluorination of 4-biphenylacetic acid (**3**) using CMB-C_3N_4.
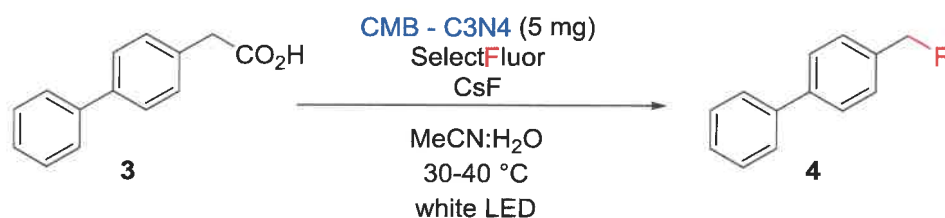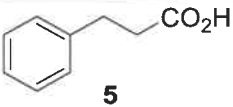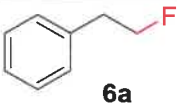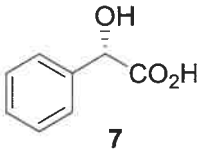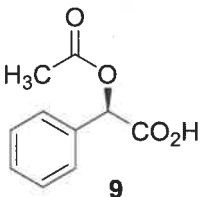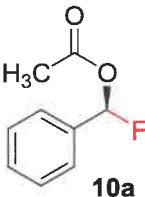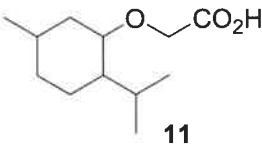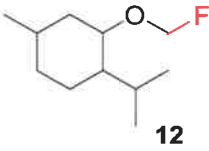

entry	irradiation time [h]	solvent ratio	NMR yield [%]	3:4
1	2		29	2.5:1
2	4	1:1	43	1.3:1
3	8		49	0.7:1
4	16		61	0.2:1
4	4	2:1	90	0.1:1
5	6		93	0

Conditions: **3** (1 equiv., 0.4 mmol), Selectfluor (3 equiv., 1.2 mmol), CsF (2 equiv., 0.8 mmol) in 3 mL of MeCN:H_2O (0.13 M). NMR yields determined by ^{19}F-NMR with α,α,α-trifluorotoluene as an internal standard and **3:4** ratios by ^{1}H-NMR according to the general procedure. Reactions performed with the first lamp.

4-(Fluoromethyl)-1,1'-biphenyl (**4**) was obtained in higher yield when the ratio of the acetonitrile:water medium was adjusted to 2:1. NMR analysis showed that under these conditions the reaction is almost complete within 4 h (Table 17, entry 4). By simply irradiating the reaction for a longer time (6 h), a quantitative consumption of the starting material was observed with an NMR yield of 93% (entry 5). The desired product (**4**) was isolated in 81% yield.

Table 19 shows the reaction scope of photocatalytic decarboxylative fluorination. The reactions below were performed using the first lamp.
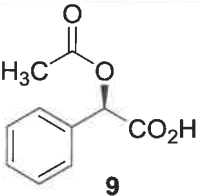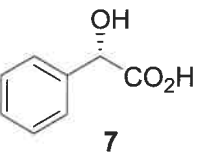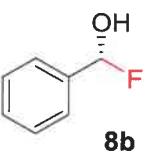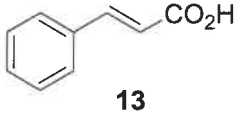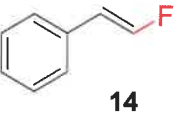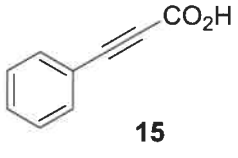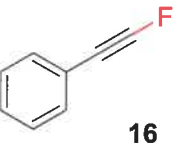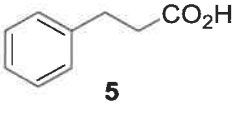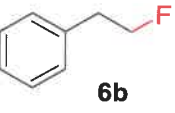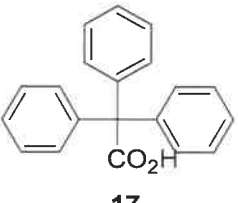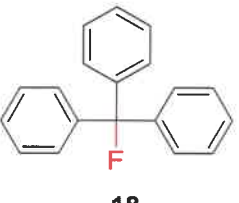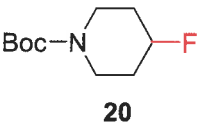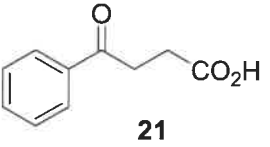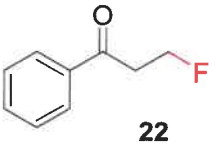
Table 19 Reaction scope for the decarboxylative fluorination performed with the first lamp.

RCO₂H	product	NMR yield [%]
5	6a	32
7	8a	0
9	10a	94
11	12	0
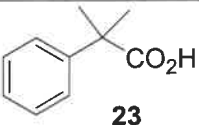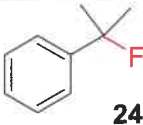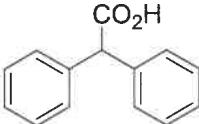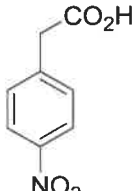
Conditions: MeCN:H₂O (1:1) was used as solvent. RCO₂H (1 equiv., 0.4 mmol), Selectfluor (3 equiv., 1.2 mmol), CsF (2 equiv., 0.8mmol) in 2 mL of MeCN:H₂O (0.2 M). NMR yields determined by ¹⁹F-NMR with α,α,α-trifluorotoluene as an internal standard by according to the general procedure. Reaction time 4 h.

Two of the four substrates resulted in the formation of the desired product (**6a** and **10a**). (S)-(+)-Mandelic acid (**7**) and (-)-Menthoxyacetic (**11**) did not work using this strategy. 3-aryl acids, such as substrate **5** (3-phenylpropionic acid) resulted in lower NMR yield than the 2-aryl acid, phenylacetic acid (2a, Table 1, entry 10) for the same reaction conditions. (S)-(+)-O-Acetylmandelic acid (**9**) was fluorinated in excellent yield (94% NMR yield).
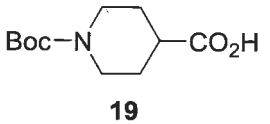
Table 20 Reaction scope for the decarboxylative fluorination performed with the second lamp.

RCO₂H	product	NMR yield [%]
9	**10b**	93
7	**8b**	0
13	**14**	50
15	**16**	0
5	**6b**	28
17	**18**	0
19	**20**	0
21	**22**	0

Table 21 Reaction scope for the decarboxylative fluorination performed with the second lamp.

RCO$_2$H	product	NMR yield [%]
23	**24**	55
25	**26**	1
27	**28**	4
29	**30**	16

Conditions: Acetonitrile/water (1:1) was used as solvent. RCO$_2$H (1 equiv., 0.4 mmol), Selectfluor (3 equiv., 1.2 mmol), CsF (2 equiv., 0.8 mmol) in 3 mL (0.13 M). NMR yields determined by ^{19}F-NMR with α,α,α-trifluorotoluene as an internal standard by according to the general procedure. Reaction time 15 h.

The substrates **7** and **9** showed the same behavior for the both lamps. A slight decrease in conversion was observed for substrate **5**. For mentioned su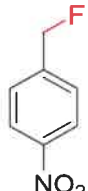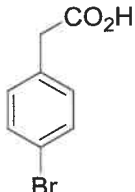bstrate (**5**), different solvent ratios of acetonitrile and water were tested (1:2 and 2:1) and resulted in similar NMR yields. Two unsaturated carboxylic acids (**13** and **15**) underwent decarboxylative fluorination with Selectfluor. The fluorination of C(sp^2) was converted to fluorinated product **14** in 50 % NMR yield. The fluorination of a sp-hybridized carbon was unsuccessful using this strategy. Notably, substrate **13**

resulted in multiple fluorination products within 24 hours and a 57 % NMR yield of **14** was observed. Triphenylacetic acid (**17**) did not result in the desired product **18** even with three different solvent ratios of acetonitrile and water (1:1, 2:1, and 3:1). Decarboxylative fluorination using CMB-C$_3$N$_4$ did not obtain desired products for unactivated carboxylic acid **19** and carboxylic acid **21**.

The desired product **24** was observed in 55 % NMR yield after decarboxylative fluorination of 2-methyl-2-phenylpropanoic acid (**23**). Furthermore, using 2,2-diphenylacetic acid (**25**) as a substrate resulted in traces of **26** by NMR (1 %). The substrate **27** with a strongly electron withdrawing group (EWG) resulted in the formation of desired product **28** in 4 % NMR yield. For substrate **29,** with the weaker EWG, the product **30** was obtained in 16 % NMR yield.

The fluorination of potassium benzyltrifluoroborate (**31**), instead of phenylacetic acid (**1**), resulted in the same fluorinated product (**32**). As summarized in Table 21, the reaction resulted in the desired product both with and without the addition of CsF within 15 hours with an NMR yield between 64 and 76 %.

Table 22 Fluorination of potassium benzyltrifluoroborate (**31**) using CMB-C$_3$N$_4$.

entry	base	NMR yield [%]
1	-	64
2	CsF	76

Conditions: **31** (1 equiv., 0.4 mmol), Selectfluor (3 equiv., 1.2 mmol), CsF (2 equiv.,0.8 mmol) in 3 mL of MeCN:H$_2$O (0.13 M). NMR yields determined by ^{19}F-NMR with α,α,α-trifluorotoluene as an internal standard by according to the general procedure. Reactions performed with the second lamp. Reaction time 15 h.

3. Conclusion

Photoredox-assisted decarboxylative fluorination has been developed for a wide range of carboxylic acid substrates. The optimal combination of base and solvent mixture was the key for this reaction. The reaction was also successful with potassium benzyltrifluoroborate (**31**) instead of phenylacetic acid (**1**) and resulted in the same fluorinated product (**2a** and **2b**). Control studies have shown that in the absence of a catalyst, light and degassing, there is no reaction. However, without a base, a very slow reaction was observed. The fluorination of $C(sp^2)$ was converted to fluorinated product **10** in 50 % NMR yield while the flluorination of $C(sp)$ **22** did not work using this strategy.

4. Experimental

4.1 General information

Substrates, reagents, and solvents were purchased from commercial suppliers and used without further purification. ^{1}H-, ^{13}C- and ^{19}F-NMR were obtained using a Varian (400 MHz) NMR spectrometer. Chemical shifts are given in parts per million (ppm). NMR data are reported in the following format: s = singlet, d = doublet, t = triplet, q = quartet, m = multiplet, with coupling constant in Hz. Purification of **4** and **10b** was carried out by flash chromatography on the Reveleris X2 Flash Chromatography System from GRACE. A prepacked column with 12 g, 40 µm silica gel was used at a 28 mL/min elution flow rate.

4.2 Preparation of CMB-C$_3$N$_4$

The CMB-C$_3$N$_4$ was prepared according to the published procedure.[48] A 1:1 cyanuric acid (**C**, 1 g): melamine (**M**) molar ratio and 0.05 molar barbituric acid (**B**) were mixed for 4 h using an automatic shaker in 40 mL of water. Then the white supramolecular complexes (**CMB***) were filtered and washed several times with water. The resulting powder was dried at 60 °C in a vacuum oven overnight and then calcined at 550 °C for 4 h under an inert nitrogen atmosphere (heating rate was 2.3 °C/min). Characterization data is in agreement with previously published data.[48]

4.3 General procedure for determining NMR yields and substrate-to-product ratios for reactions

1) 2,2,2-trifluorethanol as an internal standard

The internal standard (1 equiv.) was added and the resulting mixture was stirred for a few seconds. An aliquot (~ 0.2 mL) was removed, and analyzed by ^{19}F-NMR, (in acetone-d$_6$) to obtain NMR yields (Figure 19). The second aliquot (~ 1 mL), was transferred into a test tube and diluted with H$_2$O (~ 2 mL) and CDCl$_3$ (~ 1.5 mL). The test tube was sealed and vigorously shaken. The organic layer was carefully removed using a syringe and analyzed by ^{1}H-NMR to obtain substrate-to-product ratios (Figure 20).
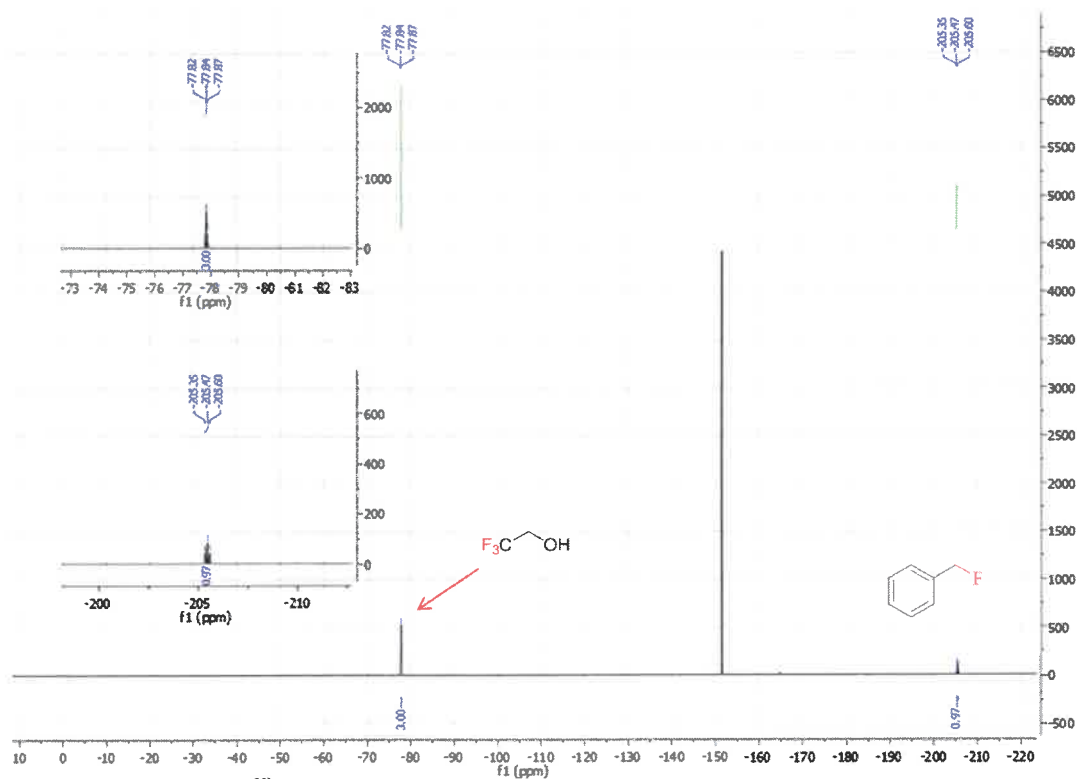
Figure 19 Example of a ^{19}F-NMR spectrum for determining NMR yields with 2,2,2-trifluorethanol. The example is taken for (Fluoromethyl)benzene (1).
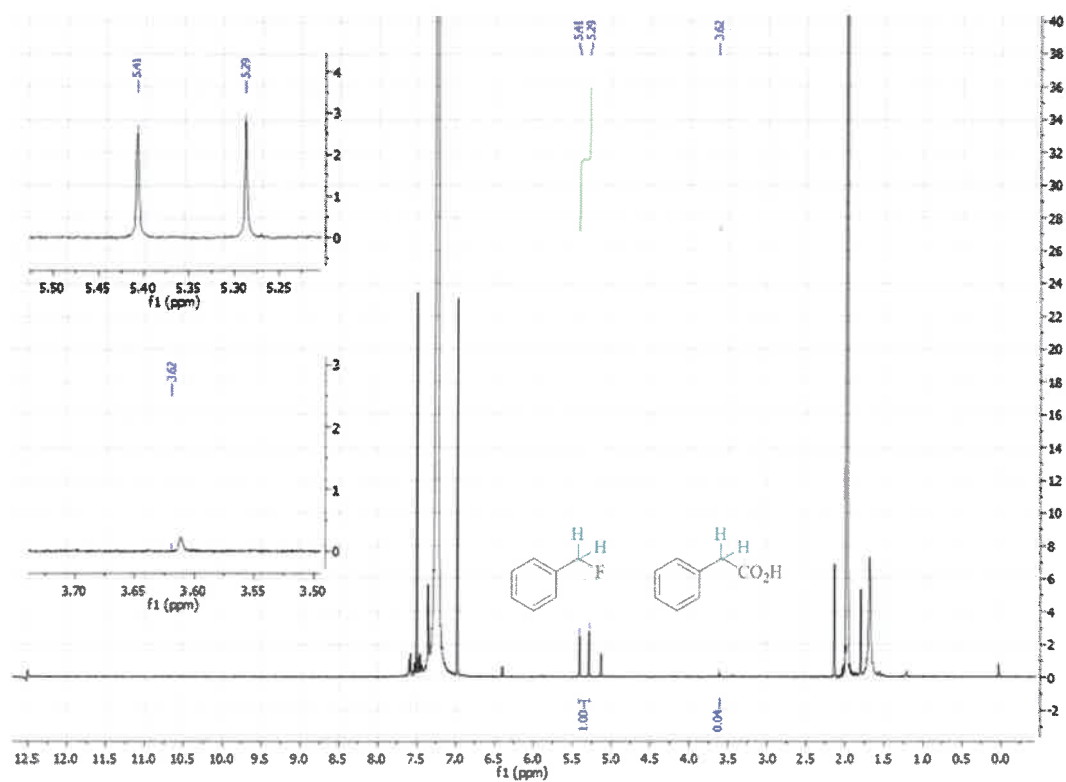
Figure 20 Example of a ^{1}H-NMR spectrum for determining substrate-to-product ratios. The example is taken for (Fluoromethyl)benzene (1).

2) α,α,α- trifluorotoluene as an internal standard

The resulting mixture was extracted with H_2O and $CDCl_3$ (3 × 10 mL). α,α,α-trifluorotoluene (1 equiv.) was added to the combined organic phases and subjected to ^{19}F-NMR (NMR yield) (Figure 21) and ^1H-NMR (substrate-to-product ratios) analysis.

Figure 21 Example of a 19F-NMR spectrum for determining NMR yields with α,α,α- trifluorotoluene. The example is taken for (Fluoromethyl)benzene (**1**).

4.4 General Procedure for Photoredox-Catalyzed Decarboxylative Fluorination of Carboxylic Acid:

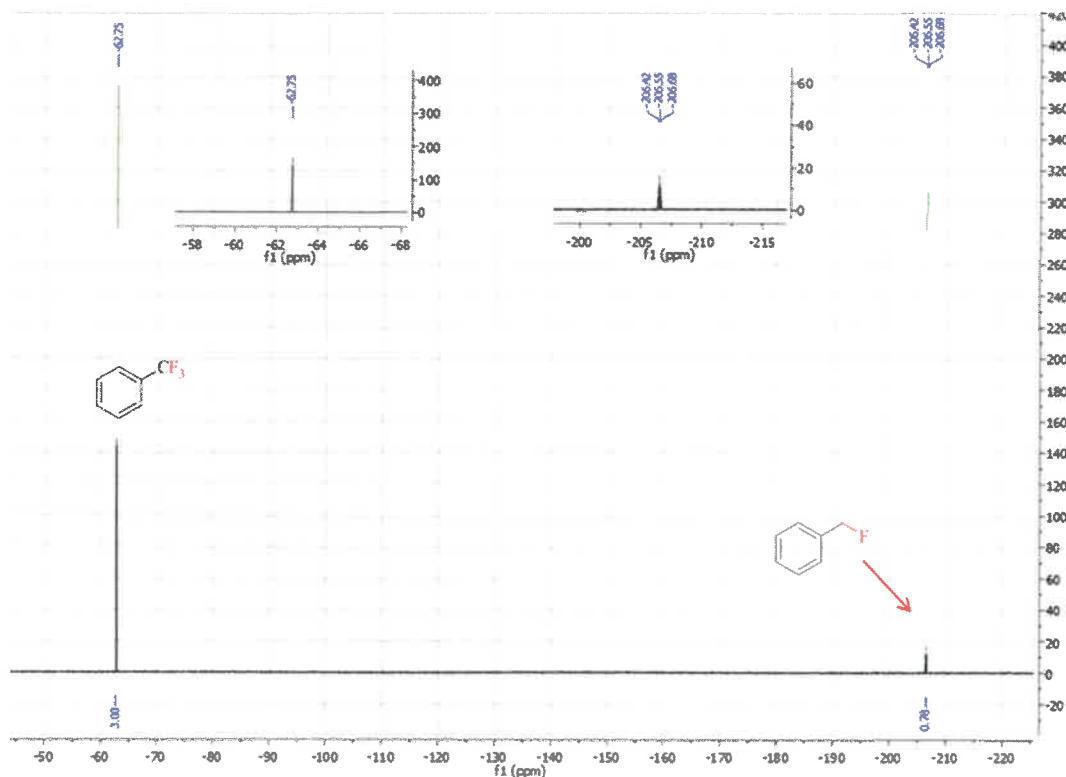An oven dried microwave vessel was equipped with a stir bar and the respective carboxylic acid (1 equiv., 0.4 mmol), CsF (2 equiv., 0.8 mmol, 121.5 mg), Selectfluor (3 equiv., 1.2 mmol, 425.1 mg) and CMB-C_3N_4 (5 mg) were added. Afterwards, the respective solvent mixture was added and the vessel was closed with a septum. The reaction mixture of acetonitrile and H_2O (3.0 ml) was stirred for 10 seconds in order to dissolve the substrate and reagents. The mixture was subsequently degassed by bubbling Argon for 10 minutes. Thereafter, the reaction mixture was irradiated with a flexible 5 meter, red/green/blue 24 W LED band in the batch reactor with rapid stirring (1400 rpm). The batch reactor was filled with water to keep up a bath temperature between 30-40 °C. The microwave vessels were placed at the same position for each experiment.

2
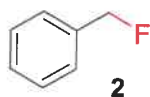
Benzyl fluoride (2):

1) According to the general procedure for the photoredox-catalyzed decarboxylative fluorination, a mixture of CMB-C_3N_4 (5 mg), phenylacetic acid (**1**) (54 mg, 0.4 mmol, 1 equiv.), CsF (122 mg, 0.8 mmol, 2 equiv.), and Selectfluor (425 mg, 1.4 mmol, 3. equiv) in acetonitrile/water (1:1) was irradiated for 15 h to obtain **2**. Analysis of the reaction mixture according to the general procedure showed 89 % NMR yield.

2) A mixture of CMB-C_3N_4 (5 mg), potassium benzyltrifluoroborate (**31**), CsF (122 mg, 0.8 mmol, 2 equiv.), and Selectfluor (425 mg, 1.4 mmol, 3. equiv) in acetonitrile/water (1:1) was irradiated for 15 h to obtain **2**. Analysis of the reaction mixture according to the general procedure showed 76 % NMR yield.

2 is a known compound and spectral data match the reported literature values.[49]

4
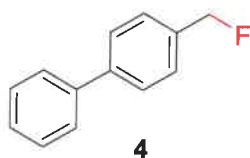
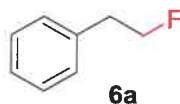**4-(Fluoromethyl)-1,1'-biphenyl (4):** According to the general procedure for the photoredox-catalyzed decarboxylative fluorination, a mixture of CMB-C_3N_4 (5 mg), 4-biphenylacetic acid (**3**) (85 mg, 0.4 mmol, 1 equiv.), CsF (122 mg, 0.8 mmol, 2 equiv.), and Selectfluor (425 mg, 1.4 mmol, 3. equiv) in acetonitrile/water (2:1) was irradiated for 6 h to obtain **4**. After the reaction completion, the crude reaction mixture was extracted with diethyl ether (Et_2O, 3 x 10 mL), the combined organic extracts were dried (Na_2SO_4) and concentrated *in vacuo*. The titled compound was isolated as a colorless oil (60.5 mg, 81 %) using the general procedure. ^1H NMR (400 MHz, Chloroform-*d*) δ 7.64 – 7.57 (m, 4H), 7.48 – 7.42 (m, 4H), 7.39 – 7.33 (m, 1H), 5.42 (d, J = 47.9 Hz, 2H). ^{13}C NMR (101 MHz, Chloroform-d) δ 141.73, 141.70, 140.57, 140.55, 135.16, 134.99, 128.81, 128.09, 128.03, 127.52, 127.36, 127.34, 127.14, 127.13, 84.40 (d, J = 165.9 Hz).^{19}F NMR (376 MHz, Chloroform-d) δ -206.15 (t, J = 47.9 Hz). **4** is a known compound and spectral data match the reported literature values.[47]

6a

2-Fluoroethylbenzene (6a): According to the general procedure for the photoredox-catalyzed decarboxylative fluorination, a mixture of CMB-C_3N_4 (5 mg), 3-phenylpropanoic acid (**5**) (60 mg, 0.4 mmol, 1 equiv.), CsF (122 mg, 0.8 mmol, 2 equiv.), and Selectfluor (425 mg, 1.4 mmol, 3. equiv) in acetonitrile/water (1:1) was irradiated for 15 h to obtain **6a**. Analysis of the reaction mixture a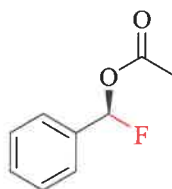ccording to the general procedure showed 32 % NMR yield. **6a** is a known compound and spectral data match the reported literature values.[50]
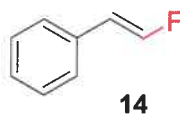

Fluoro(phenyl)methyl acetate (10b): According to the general procedure for the photoredox-catalyzed decarboxylative fluorination, a mixture of CMB-C_3N_4 (5 mg), (*S*)-(+)-*O*-Acetylmandelic acid (**9**) (78 mg, 0.4 mmol, 1 equiv.), CsF (122 mg, 0.8 mmol, 2 equiv.), and Selectfluor (425 mg, 1.4 mmol, 3. equiv) in acetonitrile/water (1:1) was irradiated for 6 h to obtain **4**. After the reaction completion, the crude reaction mixture was extracted with diethyl ether (Et$_2$O, 3 x 10 mL), the combined organic extracts were dried (Na$_2$SO$_4$) and concentrated *in vacuo*. The titled compound was isolated as a colorless oil (53 mg, 86 %) using the general procedure. ^{19}F NMR (376 MHz, Chloroform-d) δ -122.33 (d, J = 55.1 Hz).

14

(E)-(2-Fluorovinyl)benzene (14): According to the general procedure for the photoredox-catalyzed decarboxylative fluorination, a mixture of CMB-C_3N_4 (5 mg), (2E)-3-phenylprop-2-enoic acid (**13**) (59 mg, 0.4 mmol, 1 equiv.), CsF (122 mg, 0.8 mmol, 2 equiv.), and Selectfluor (425 mg, 1.4 mmol, 3. equiv) in acetonitrile/water (1:1) was irradiated for 15 h to obtain **14**. Analysis of the reaction mixture according to the general procedure showed 50 % NMR yield. **14** is a known compound and spectral data match the reported literature values.[51]
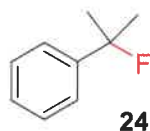

24

(2-Fluoropropan-2-yl)benzene (24): According to the general procedure for the photoredox-catalyzed decarboxylative fluorination, a mixture of CMB-C_3N_4 (5 mg), 2-methyl-2-phenylpropanoic acid (**23**) (66 mg, 0.4 mmol, 1 equiv.), CsF (122 mg, 0.8 mmol, 2 equiv.), and Selectfluor (425 mg, 1.4 mmol, 3. equiv) in acetonitrile/water (1:1) was irradiated for 15 h to obtain **24**. Analysis of the reaction mixture according to the general procedure showed 55 % NMR yield. **24** is a known compound and spectral data match the reported literature values.[52]
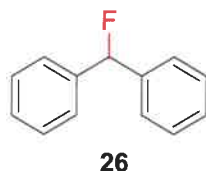
26

(Fluoromethylene)dibenzene (26): According to the general procedure for the photoredox-catalyzed decarboxylative fluorination, a mixture of CMB-C$_3$N$_4$ (5 mg), 2-methyl-2-phenylpropanoic acid (**25**) (85 mg, 0.4 mmol, 1 equiv.), CsF (122 mg, 0.8 mmol, 2 equiv.), and Selectfluor (425 mg, 1.4 mmol, 3. equiv) in acetonitrile/water (1:1) was irradiated for 16 h to obtain **26**. Analysis of the reaction mixture according to the general procedure showed 1 % NMR yield. **26** is a known compound and spectral data match the reported literature values.[53]

NO$_2$

28

4-Nitrobenzyl fluoride (28): According to the general procedure for the photoredox-catalyzed decarboxylative fluorination, a mixture of CMB-C$_3$N$_4$ (5 mg), 2-(4-nitrophenyl)acetic acid (**27**) (72.5 mg, 0.4 mmol, 1 equiv.), CsF (122 mg, 0.8 mmol, 2 equiv.), and Selectfluor (425 mg, 1.4 mmol, 3. equiv) in acetonitrile/water (1:1) was irradiated for 16 h to obtain 28. Analysis of the reaction mixture according to the general procedure showed 4 % NMR yield. 28 is a known compound and spectral data match the reported literature values.[54]

30

4-Bromobenzyl fluoride (30): According to the general procedure for the photoredox-catalyzed decarboxylative fluorination, a mixture of CMB-C_3N_4 (5 mg), 2-(4-bromophenyl)acetic acid (**29**) (86 mg, 0.4 mmol, 1 equiv.), CsF (122 mg, 0.8 mmol, 2 equiv.), and Selectfluor (425 mg, 1.4 mmol, 3. equiv) in acetonitrile/water (1:1) was irradiated for 16 h to obtain 30. Analysis of the reaction mixture according to the general procedure showed 16 % NMR yield. 30 is a known compound and spectral data match the reported literature values.[54]

5. References

1. McNaught, A. D.; McNaught, A. D., *Compendium of chemical terminology.* Blackwell Science Oxford: 1997; Vol. 1669.

2. Glusac, K. What has light ever done for chemistry? Nature Research, 2016.

3. Ekambaram, S., *General chemistry.* Pearson Education India: 2005.

4. Shaw, M. H.; Twilton, J.; MacMillan, D. W., *The Journal of organic chemistry* **2016,** *81* (16), 6898-6926.

5. Prier, C. K.; Rankic, D. A.; MacMillan, D. W., *Chemical reviews* **2013,** *113* (7), 5322-5363.

6. Takeda, H.; Ishitani, O., *Coordination Chemistry Reviews* **2010,** *254* (3), 346-354.

7. Graetzel, M., *Accounts of Chemical Research* **1981,** *14* (12), 376-384.

8. Kalyanasundaram, K.; Grätzel, M., *Coordination chemistry reviews* **1998,** *177* (1), 347-414.

9. Stephan, D. W., *J. Am. Chem. Soc* **2015,** *137* (32), 10018-10032.

10. Burns, M.; Essafi, S.; Bame, J. R.; Bull, S. P.; Webster, M. P.; Balieu, S.; Dale, J. W.; Butts, C. P.; Harvey, J. N.; Aggarwal, V. K., *Nature* **2014,** *513* (7517), 183.

11. Lovering, F.; Bikker, J.; Humblet, C., *Journal of medicinal chemistry* **2009,** *52* (21), 6752-6756.

12. Brown, D. G.; Boström, J., *J. Med. Chem* **2016,** *59* (10), 4443-4458.

13. Hofbeck, T.; Yersin, H., *Inorganic chemistry* **2010,** *49* (20), 9290-9299.

14. Romero, N. A.; Nicewicz, D. A., *Chemical reviews* **2016,** *116* (17), 10075-10166.

15. Bryan Sears, R.; Joyce, L. E.; Turro, C., *Photochemistry and photobiology* **2010,** *86* (6), 1230-1236.

16. Ram, R. N.; Manoj, T., *The Journal of organic chemistry* **2008,** *73* (14), 5633-5635.

17. Ardo, S.; Meyer, G. J., *Chemical Society Reviews* **2009,** *38* (1), 115-164.

18. Juris, A.; Balzani, V.; Barigelletti, F.; Campagna, S.; Belser, P. I.; Von Zelewsky, A., *Coordination Chemistry Reviews* **1988,** *84*, 85-277.

19. Kumar, R. S.; Kulangiappar, K.; Kulandainathan, M. A., *Synthetic Communications®* **2010,** *40* (12), 1736-1742.

20. Cismesia, M. A.; Ischay, M. A.; Yoon, T. P., *Synthesis* **2013,** *45* (19), 2699-2705.

21. Zhu, S.; Das, A.; Bui, L.; Zhou, H.; Curran, D. P.; Rueping, M., *Journal of the American Chemical Society* **2013,** *135* (5), 1823-1829.

22. Hari, D. P.; Schroll, P.; König, B., *Journal of the American Chemical Society* **2012,** *134* (6), 2958-2961.

23. Xie, J.; Jin, H.; Xu, P.; Zhu, C., *Tetrahedron Letters* **2014,** *55* (1), 36-48.

24. Zhang, Y.; Crittenden, J. C.; Hand, D. W.; Perram, D. L., *Environmental science & technology* **1994,** *28* (3), 435-442.

25. Hoffmann, M. R.; Martin, S. T.; Choi, W.; Bahnemann, D. W., *Chemical reviews* **1995,** *95* (1), 69-96.

26. Schiavello, M.; Sclafani, A., *Photocatalysis: Fundamentals and Applications. John Wiley & Sons* **1989,** 159-173.

27. Serpone, N.; Lawless, D.; Pelizzetti, E., Subnanosecond characteristics and photophysics of nanosized TiO2 particulates from Rpart= 10 A to 134 A: Meaning for heterogeneous Photocatalysis. In *Fine Particles Science and Technology*, Springer: 1996; pp 657-673.

28. Baar, M.; Blechert, S., *Chemistry-A European Journal* **2015,** *21* (2), 526-530.

29. Zheng, Q.; Durkin, D. P.; Elenewski, J. E.; Sun, Y.; Banek, N. A.; Hua, L.; Chen, H.; Wagner, M. J.; Zhang, W.; Shuai, D., *Environmental science & technology* **2016,** *50* (23), 12938-12948.

30. Zhang, Z.; Lu, B.; Hao, J.; Yang, W.; Tang, J., *Chemical communications* **2014,** *50* (78), 11554-11557.

31. Zheng, Y.; Liu, J.; Liang, J.; Jaroniec, M.; Qiao, S. Z., *Energy & Environmental Science* **2012,** *5* (5), 6717-6731.

32. Zhang, Y.; Mori, T.; Ye, J.; Antonietti, M., *Journal of the American Chemical Society* **2010,** *132* (18), 6294-6295.

33. Gallezot, P., *Chemical Society Reviews* **2012,** *41* (4), 1538-1558.

34. Jin, Y.; Fu, H., *Asian Journal of Organic Chemistry* **2017,** *6* (4), 368-385.

35. Purser, S.; Moore, P. R.; Swallow, S.; Gouverneur, V., *Chemical Society Reviews* **2008,** *37* (2), 320-330.

36. Müller, K.; Faeh, C.; Diederich, F., *Science* **2007,** *317* (5846), 1881-1886.

37.   Beeson, T. D.; MacMillan, D. W., *Journal of the American Chemical Society* **2005,** *127* (24), 8826-8828.

38.   Liu, W.; Huang, X.; Cheng, M.-J.; Nielsen, R. J.; Goddard, W. A.; Groves, J. T., *Science* **2012,** *337* (6100), 1322-1325.

39.   Liu, W.; Groves, J. T., *Angewandte Chemie International Edition* **2013,** *52* (23), 6024-6027.

40.   Tang, P.; Wang, W.; Ritter, T., *Journal of the American Chemical Society* **2011,** *133* (30), 11482-11484.

41.   Ye, Y.; Schimler, S. D.; Hanley, P. S.; Sanford, M. S., *Journal of the American Chemical Society* **2013,** *135* (44), 16292-16295.

42.   Fier, P. S.; Luo, J.; Hartwig, J. F., *Journal of the American Chemical Society* **2013,** *135* (7), 2552-2559.

43.   Watson, D. A.; Su, M.; Teverovskiy, G.; Zhang, Y.; García-Fortanet, J.; Kinzel, T.; Buchwald, S. L., *Science* **2009,** *325* (5948), 1661-1664.

44.   Maimone, T. J.; Milner, P. J.; Kinzel, T.; Zhang, Y.; Takase, M. K.; Buchwald, S. L., *Journal of the American Chemical Society* **2011,** *133* (45), 18106-18109.

45.   Yin, F.; Wang, Z.; Li, Z.; Li, C., *Journal of the American Chemical Society* **2012,** *134* (25), 10401-10404.

46.   Rueda-Becerril, M.; Mahe, O.; Drouin, M.; Majewski, M. B.; West, J. G.; Wolf, M. O.; Sammis, G. M.; Paquin, J.-F., *Journal of the American Chemical Society* **2014,** *136* (6), 2637-2641.

47.   Ventre, S.; Petronijevic, F. R.; MacMillan, D. W., *Journal of the American Chemical Society* **2015,** *137* (17), 5654-5657.

48.   Shalom, M.; Guttentag, M.; Fettkenhauer, C.; Inal, S.; Neher, D.; Llobet, A.; Antonietti, M., *Chemistry of Materials* **2014,** *26* (19), 5812-5818.

49.   Leung, J. C.; Chatalova-Sazepin, C.; West, J. G.; Rueda-Becerril, M.; Paquin, J. F.; Sammis, G. M., *Angewandte Chemie International Edition* **2012,** *51* (43), 10804-10807.

50.   Kondo, Y.; Shilai, M.; Uchiyama, M.; Sakamoto, T., *Journal of the American Chemical Society* **1999,** *121* (14), 3539-3540.

51.   Landelle, G. g.; Turcotte-Savard, M.-O.; Angers, L.; Paquin, J.-F. o., *Organic letters* **2011,** *13* (6), 1568-1571.

52.   Adcock, W.; Abeywickrema, A., *Australian Journal of Chemistry* **1980,** *33* (1), 181-187.

53.   Wu, X.; Meng, C.; Yuan, X.; Jia, X.; Qian, X.; Ye, J., *Chemical Communications* **2015**, *51* (59), 11864-11867.

54.   Blessley, G.; Holden, P.; Walker, M.; Brown, J. M.; Gouverneur, V., *Organic letters* **2012,** *14* (11), 2754-2757.

6. Appendix

4-(Fluoromethyl)-1,1'-biphenyl (4)
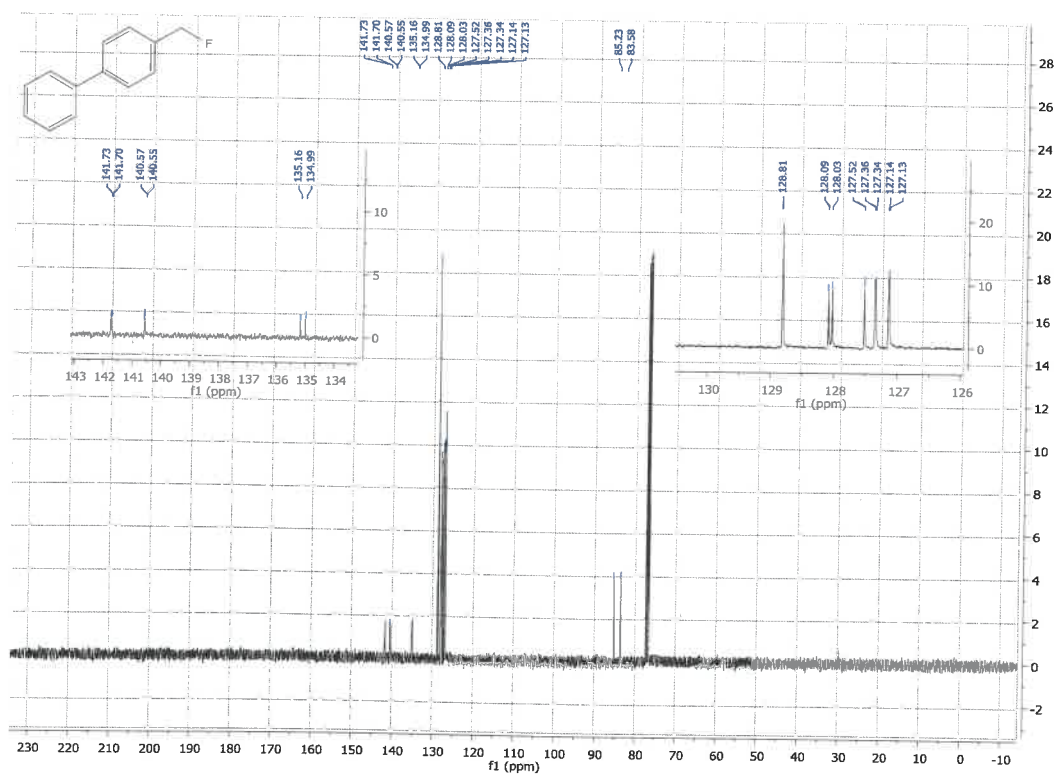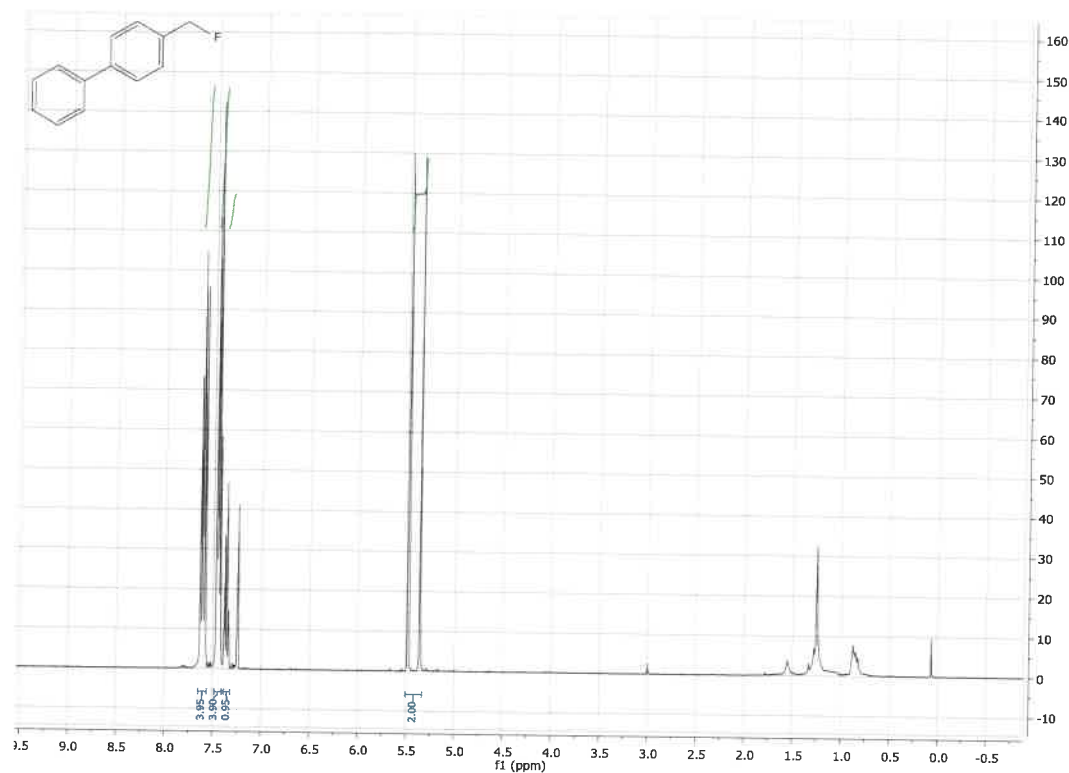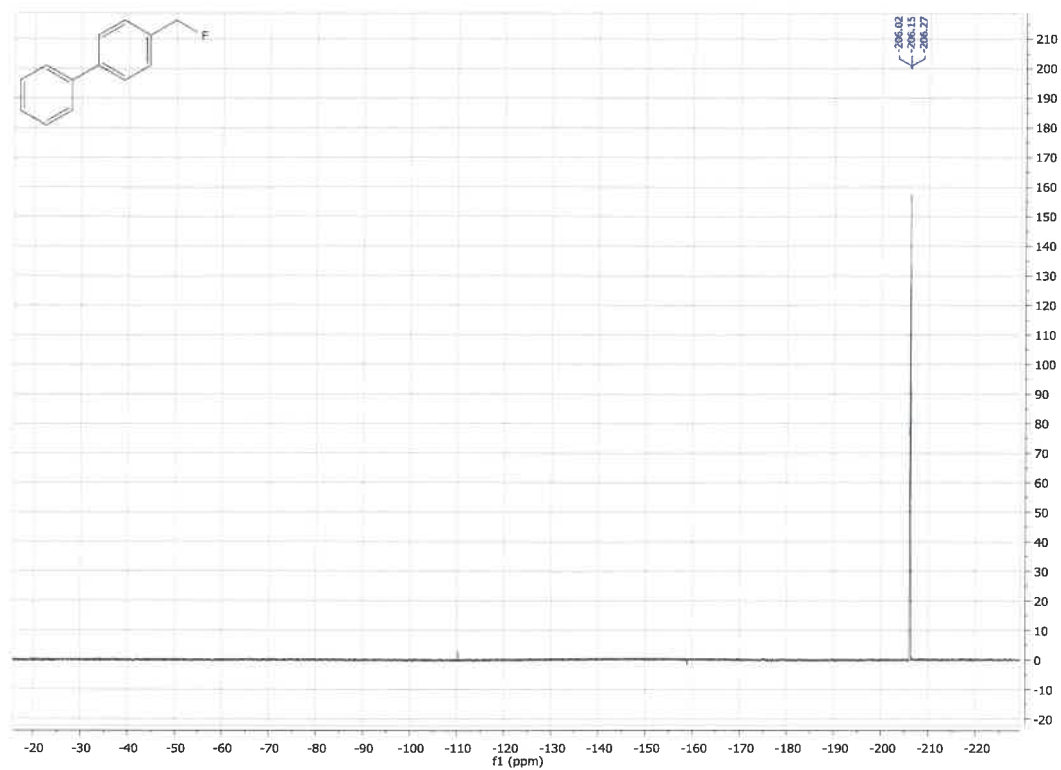
Fluoro(phenyl)methyl acetate (10b)
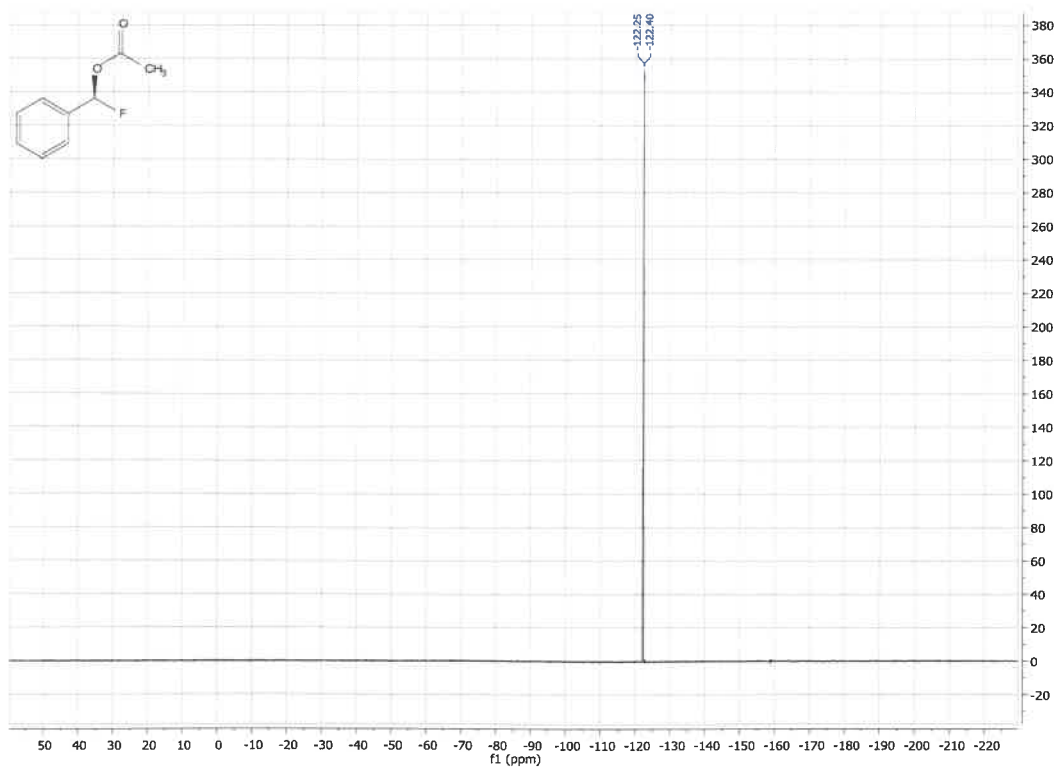
Curriculum vitae

Education

2015-2017
(Expected)

Master of Science, Applied Chemistry
Faculty of Chemical Engineering and Technology, University of Zagreb, Zagreb (Croatia)

2011-2015

Bachelor of Science, Applied Chemistry
Faculty of Chemical Engineering and Technology, University of Zagreb, Zagreb (Croatia)
Supervisor: Prof. Silvana Raić – Malić
Bachelor's thesis: *L*-ascorbic Acid and its Derivatives.

Research Experience

03/2017-09/2017

Master Thesis Student
Max Planck Institute of Colloids and Interfaces, Potsdam (Germany)
Supervisor: Dr. Kerry Gilmore
Master's thesis: *Novel Heterogeneous Photoredox Transformations Using Organic Materials.*

07/2015-10/2015

Research Internship
University of Namur, Unit of Organic Chemistry, NAmur MEdicine & Drug Innovation Center (NAMEDIC), Namur (Belgium)
Supervisor: Dr. Eduard Dolušić
Project: Flow Synthesis of Combretastatine A-4.

02/2014-06/2015

Student Researcher
Faculty of Chemical Engineering and Technology, Department of Organic Chemistry, University of Zagreb, Zagreb (Croatia)
Project leader: Prof. Silvana Raić – Malić
Project:Synthesis and Cytostatic Evaluations of NovEl Nitrogen heTeRocycles librarY (SCIENcENTRY).

09/2014-10/2014

Student Researcher
Ruđer Bošković Institute, Division of Organic Chemistry and Biochemistry, Zagreb (Croatia)
Supervisor: Dr. Lidija Varga – Defterdarović
Project:Synthesis of Octapeptides and Disaccharides.

Academic Honours

- Deutscher Akademischer Austauschdienst (DAAD) Research Scholarship for a 4 month stay in the group of Prof. Peter H. Seeberger at Max Planck Institute of Colloids and Interfaces, Germany (2017).

Conferences

- **I. Cazin**, I. Kovačić, A. Meščić, V. Stepanić, S. Raić-Mailć, 1,2,3-triazole appended *L*-ascorbic acid with antioxidant properties // XXIV Croatian Meeting of Chemists and Chemical Engineers, Croatian Society of Chemical Engineers/Croatian Chemical Society, 2015, (poster).
- **I. Cazin**, E. Dolušić, S. Lanners, Flow synthesis of combretastatine A-4 // Fourth Conference of Young Chemists of Serbia, Belgrade, Serbia, 2016, (poster).
- **I. Cazin**, E. Dolušić, S. Lanners, Flow synthesis of combretastatine A-4 // Third Student Symposium, Zagreb, Croatia, 2016, (oral presentation).

Skills

Job-related skills: Organic synthetic chemistry, Medicinal chemistry, Flow chemistry, Photochemistry
Preparation, isolation and characterization of organic molecules; working under oxygen-free conditions
Instrumentation experience: MW assisted synthesis, continuous flow and microreactor technology, NMR spectrometry, cyclic voltammetry.

Computer skills: Microsoft Office (Word, Excel, PowerPoint), ChemDraw, MestreNova, SciFinder.

References

Prof. Dr. Peter H. Seeberger
Max Planck Institute of
Colloids and Interfaces
Am Mühlenberg 1,
14476, Potsdam-Golm,
Germany
peter.seeberger@mpikg.mpg.de

**Prof. Silvana Raić –
Malić**
Faculty of Chemical
Engineering and
Technology
HR-10000 Zagreb,
Croatia
sraic@fkit.hr

Dr. Eduard Dolušić
University of Namur
Rue de Bruxelles 61,
B-5000
Namur, Belgium
eduard.dolusic@unamur.be